Biodegradation of diluted bitumen in shallow groundwater systems

Leah Mindorff

Department of Earth and Planetary Sciences

McGill University

Montreal, QC, Canada

April 2022

A thesis submitted to the Faculty of Graduate Studies and Research in partial fulfilments of the requirements for the degree of Master of Science

Table of Contents

Acknowledgements

Throughout the undertaking of this thesis project I have received a great deal of support for which I am very grateful.

First and foremost, I would like to thank my supervisors Dr. Nagissa Mahmoudi and Dr. Jason Ahad. Their expertise and guidance throughout my masters' have been invaluable and I am deeply grateful to them for giving me this opportunity.

Many thanks as well to all the members of the Delta Lab over the past two years (Jade Bergeron, Scott Hepditch, Josué Jautzy, Marc Luzincourt, Joëlle Marion, Hooshang Pakdel, Anna Smirnoff) for offering their valuable advice, insight and technical support.

Finally, I would like to thank my friends and family for their endless encouragement and support. I could not have done it without them.

Contributions of Authors

This thesis is comprised of original research conducted by Leah Mindorff at the Department of Earth and Planetary Sciences, McGill University and at the Delta Lab, Geological Survey of Canada-Quebec under the co-supervision of Dr. Nagissa Mahmoudi and Dr. Jason ME Ahad. This thesis is based on a single manuscript intended for publication in a peer-reviewed journal with Leah Mindorff as the first author and Jason M.E. Ahad, Nagissa Mahmoudi, Scott Hepditch, Valerie Langlois, and Richard Martel as co-authors. The data for this thesis was generated from an experiment run over a 104-day period in the summer and fall of 2019. Sample extraction, analysis and data interpretation were conducted between 2019 and 2021. All co-authors contributed intellectually and assisted with the experimental design, sample collection, sample analysis, and/or data interpretation. Thesis drafts were prepared and revised by Leah Mindorff based on recommendations and edits from Dr. Nagissa Mahmoudi and Dr. Jason M.E. Ahad.

List of Figures

Abstract

The oil sands region in Western Canada is one of the world's largest proven oil reserves. To facilitate pipeline transport, highly viscous oil sands bitumen is blended with lighter hydrocarbon fractions to produce diluted bitumen (dilbit). With anticipated increases in bitumen production and transport dilbit, the risk of a dilbit spill is expected to rise. To understand the behaviour of dilbit in shallow groundwater systems in the event of a spill, we ran side-by-side dilbit and conventional heavy crude exposures, along with an untreated control, using soil-filled mesocosms. Soil cores were taken from the three mesocosm treatments at set intervals during a 104-day exposure. Phospholipid fatty acids (PLFAs), biomarkers for the active microbial population, were extracted from the soil. The stable carbon isotope ($\delta^{13}C$) contents of individual PLFAs and the radiocarbon contents ($\Delta^{14}C$) of bulk PLFAs were then characterized. The $\Delta^{14}C$ of bulk PLFAs ranged from -221.1‰ to -54.7‰ and -259.4‰ to -107.1‰ in dilbit- and conventional heavy crude-affected samples, respectively, indicating similar levels of microbial uptake of both oils compared to control soils ($\Delta^{14}C$-PLFA values > -46.1‰). 16S ribosomal RNA genes were also extracted from the mesocosm soil cores. Amplicon sequencing revealed that the microbial communities changed over time and these changes were different between treatment types. The relative abundance of *Polaromonas*, a known hydrocarbon-degrading bacterial genus, was significantly increased following exposure to both dilbit- and conventional crude-contaminated soil. This study demonstrates that the biodegradability of dilbit by the native microbial community following a spill in the shallow subsurface is similar to that of conventional heavy crude oil.

Resumé

La région des sables bitumineux de l'Ouest canadien est l'une des plus grandes réserves prouvées de pétrole au monde. Pour faciliter le transport par pipeline, le bitume des sables bitumineux très visqueux est mélangé à des fractions d'hydrocarbures plus légères pour produire du bitume dilué (dilbit). Avec les augmentations prévues de la production de bitume et du transport de dilbit, le risque de déversement de dilbit devrait augmenter. Pour comprendre le comportement du dilbit dans les systèmes d'eaux souterraines peu profondes en cas de déversement, nous avons effectué des expositions côte à côte au dilbit et au brut lourd conventionnel, ainsi qu'un contrôle non traité, en utilisant des mésocosmes remplis de sol. Des carottes de sol ont été prélevées des trois traitements en mésocosme à des intervalles définis au cours d'une exposition de 104 jours. Des acides gras phospholipidiques (AGP), biomarqueurs de la population microbienne active, ont été extraits du sol. Les teneurs en isotopes stables du carbone ($\delta^{13}C$) des AGP individuels et les teneurs en radiocarbone ($\Delta^{14}C$) des AGP en vrac ont ensuite été caractérisées. Le ^{14}C des AGPL en vrac variait de -221,1 à -54,7‰ et de -259,4 à -107,1‰ dans les échantillons affectés par le dilbit et le brut lourd conventionnel, respectivement, indiquant des niveaux similaires d'absorption microbienne des deux huiles par rapport aux sols témoins ($\Delta^{14}C$ -Valeurs AGP > -46,1‰). Des gènes d'ARN ribosomique 16S ont également été extraits des carottes de sol du mésocosme. Le séquençage d'amplicon a révélé que les communautés microbiennes ont changé au fil du temps et que ces changements étaient différents entre les types de traitement. L'abondance relative de *Polaromonas*, un genre bactérien connu pour la dégradation des hydrocarbures, a augmenté de manière significative après une exposition à des sols contaminés par du dilbit et du brut lourd conventionnel. Cette étude démontre que la biodégradabilité du

dilbit par la communauté microbienne indigène à la suite d'un déversement dans le sous-sol peu profond est similaire à celle du pétrole brut lourd conventionnel.

CHAPTER 1: Literature Review

1.1. Alberta's Oil Sands

Crude oil is a naturally occurring mixture of hydrocarbons produced from the transformation of buried of organic material under high temperatures and pressures over millions of years (Strausz and Lown, 2003). The geological conditions under which a deposit is formed directly affect the chemical and physical properties of the crude oil. In turn, this impacts the methods required to extract and refine the crude oil. Conventional crude oil deposits may be extracted using typical oil wells. Unconventional methods such as hydraulic fracturing, mining, and in situ steam extraction may be employed for less accessible crude oil deposits. After recovery crude oil is transported by pipeline, ship, or railway to refineries where it can be processed into everyday products such as transportation fuels, petrochemical feedstocks, and asphalt (CAPP, 2020). Globally, the utilization of these products has steadily risen, leading to the depletion of conventional crude oil sources, and a greater interest in exploiting unconventional crude oil sources (CAPP, 2020).

Alberta's oil sands represent the world's third-largest known crude oil reserves and play an important role in Canada's economy (Government of Canada, 2016). Unlike conventional heavy crude oil deposits, the oil extracted from Alberta is a highly degraded, viscous form of petroleum known as bitumen (Figure 1). The unique physical properties of oil sands bitumen require unconventional extraction methods that demand more complex technology and higher production costs (Government of Canada, 2016). Despite these added difficulties, increases in production and transportation of bitumen are expected to continue in coming decades (CAPP, 2020).

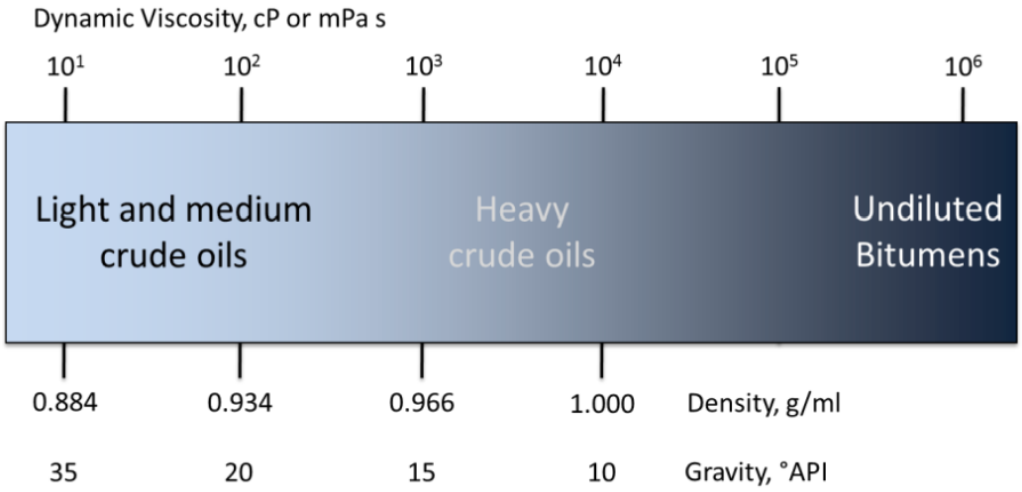

Figure 1. Crude oil varieties arranged on a spectrum based on their viscosity, density and API gravity (Lee et al., 2015).

1.2. Chemical Composition of Diluted Bitumen

The major chemical constituents of all crude oils can be grouped into four main structural classes: saturates, aromatics, resins, and asphaltenes (Lee *et al.*, 2015; National Academies of Sciences, 2016). Composition in terms of weight percent of these structural classes in conventional crude oil as compared to dilbit blends (Cold Lake Blend and Western Canadian Select) are represented in Figure 2. The relative abundances of these classes directly impact the physical and chemical properties of the crude oil and large variations result in different types of crude oils. Saturated hydrocarbons are, for most crude oils, the most abundant chemical class. These are saturated straight chain, branched chain or ringed alkane structures characterized by their low density, low viscosity, and high biodegradability. Their relative proportions decrease moving from the light crude oils to the more degraded, heavier crude oils and bitumen (King et al., 2017). Aromatic hydrocarbon structures are either based on a single benzene ring, as seen in the case of the BTEX series (benzene, toluene, ethylbenzene, and xylene isomers), or on multiple fused benzene rings, as in the case of the polycyclic aromatic hydrocarbons (PAHs). Asphaltenes and resins are structurally similar but asphaltenes have higher molecular weights

and are more polyaromatic. Together, resins and asphaltenes comprise a highly recalcitrant fraction of petroleum compounds (Atlas, 1981). They are characteristic of heavy crudes and bitumen and contribute to their high viscosity and density (Huang et al., 2019; Spalding and Hirsh, 2012). In addition to these four major classes, there are several other minor constituents of crude oil that exist such as sulphur, metals, organometals, naphthenic acids, and mineral particles. These are often associated with high asphaltene and resin content and are therefore abundant in bitumen products (National Academies of Sciences, 2016; Radović et al., 2018).

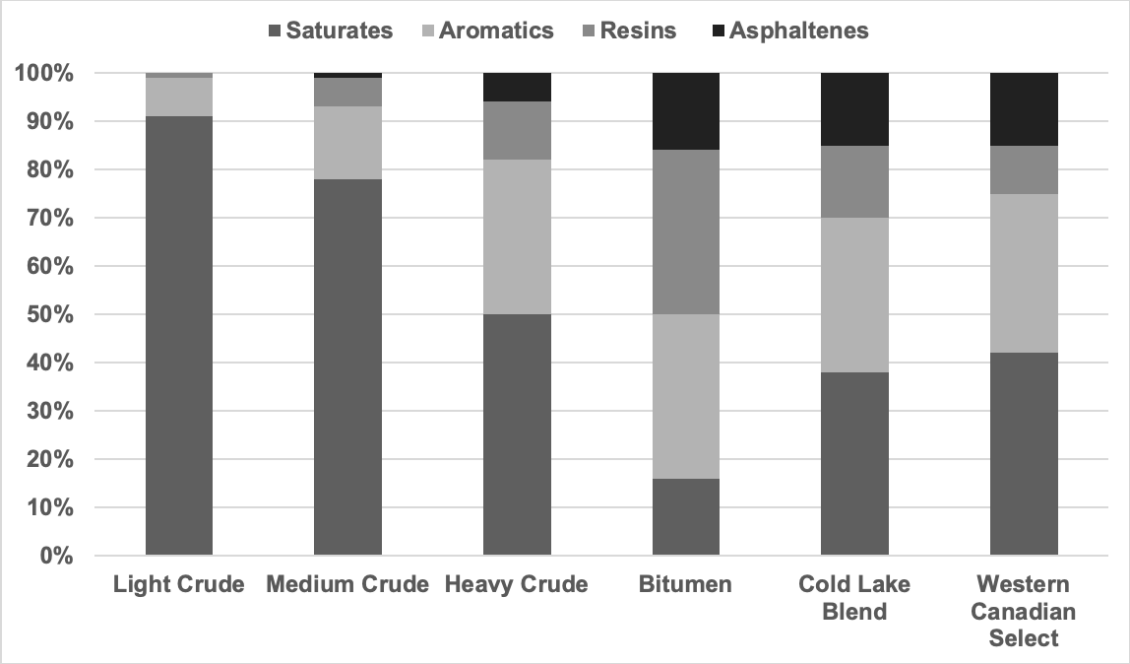

Figure 2. Percent weight of crude oil components according to crude oil type (National Academy of Science, Engineering, and Mathematices, 2016).

The high aromatic, asphaltene and resin content of bitumen make it is too dense and viscous to be pumped through a pipeline. To facilitate its transport, bitumen is blended with lighter hydrocarbon fractions (diluents) to yield a less viscous mixture of diluted bitumen (Crosby et al., 2013; National Academies of Sciences, 2016; Radović *et al.*, 2018). Diluents are typically natural gas condensates, naphtha, or other light hydrocarbons. While a number of

diluted bitumen blends exist, ‘dilbit’ is by far the most common. It is typically manufactured at a ratio of 70-80% bitumen to 20-30% diluent (CAPP, 2020; Crosby *et al.*, 2013; Spalding and Hirsh, 2012). Blends are made at the producer’s discretion and large variations in the types and relative proportions of diluents, as well as the regional differences in bitumen quality, mean that the exact chemical nature of diluted bitumen is not clearly defined. This makes predicting their behaviour in the environment even more challenging (Lee *et al.*, 2015; Spalding and Hirsh, 2012).

1.3. The Fate of Spilled Dilbit in Shallow Groundwater Systems

An estimated 3.9 million barrels per day flowed through Western Canadian pipelines in 2019, with over 840,000 km of pipeline networks crossing the country. The risk of inland oil spill is undoubtedly present and there is potential for spills to affect a wide range of freshwater, terrestrial, and groundwater systems (NRCan, 2020). Compared to marine spills, inland spills are in many ways of greater concern as they have a greater potential to occur near populated areas, affect drinking water supplies, and affect environments with a much lower capacity to dilute and disperse the oil (Lee *et al.*, 2015; Owens et al., 1993). Soils and shallow groundwater systems, despite being the environment most frequently impacted by pipeline ruptures, have received much less attention compared to surface freshwater and marine environments (Owens *et al.*, 1993; Zhao et al., 2021).

1.3.1. Abiotic Weathering

Once dilbit is released into the environment a combination of physical, chemical and biological weathering processes act on it (Figure 3). Weathering starts immediately following a spill with the lightest hydrocarbon components, present in the diluent, which will quickly volatilize (Ng et

al., 2015). BTEX hydrocarbons and other water-soluble compounds not lost to volatilization may leach into groundwater and migrate down the flow gradient (Essaid et al., 2011; Spalding and Hirsh, 2012). Soil characteristics and water table depth are among the many environmental factors deciding the potential for a spill body to migrate into groundwater systems. The loss of smaller hydrocarbon fractions through volatilization and leaching disproportionally increases the relative abundance of heavy resins and asphaltenes of dilbit compared to conventional crude oils. This in turn leads to dramatic changes in the physical properties of the residual dilbit (Lewan et al., 2014; Pesarini et al., 2010; Stoyanovich et al., 2019). Following initial weathering processes, downward mobility of the remaining dense, viscous fractions of dilbit would be limited as these highly adhesive fractions typically become trapped in soil pores in the unsaturated zone (Huang *et al.*, 2019; Lee et al., 2012; Ramseur et al., 2012).

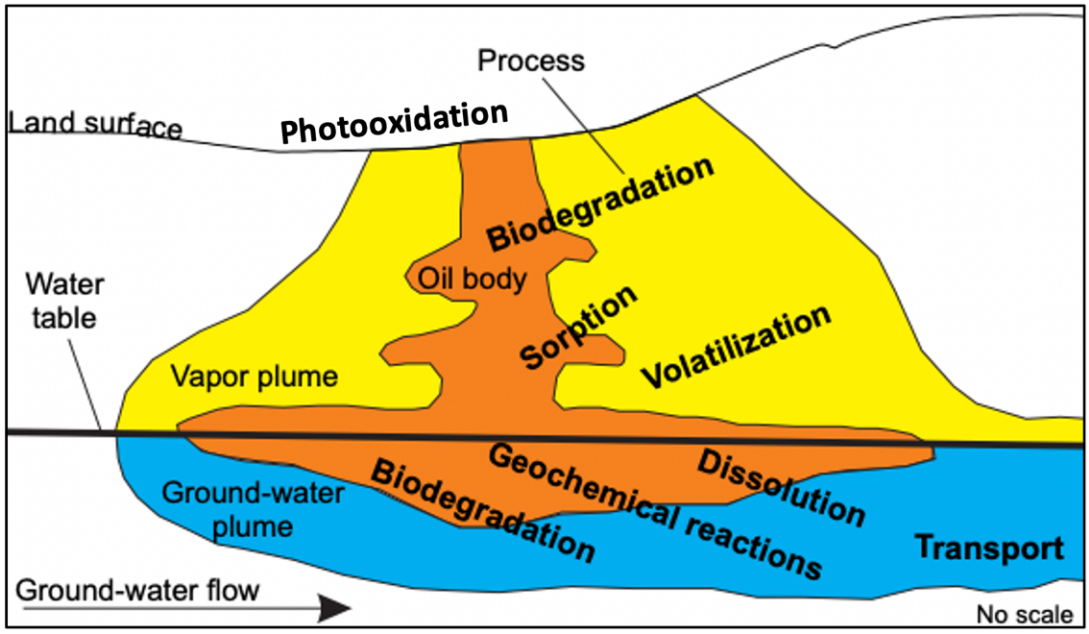

Figure 3. A conceptual model of oil degradation pathways (modified from Essaid *et al.*, 2011; Ng et al., 2015).

1.3.2. Biodegradation

In addition to the abiotic weathering that takes place following a spill, biodegradation of conventional crude oils by local microbial communities has been widely studied and is known to play an important role in the remediation of crude oil spills (Figure 3). Microorganisms adapted to degrading petroleum hydrocarbons are ubiquitous across all environments and all domains of life (Atlas and Hazen, 2011; Widdel et al., 2010). When a crude oil spill occurs, hydrocarbon-degraders, which may have made up only a small proportion of the community prior to the spill, increase in abundance thereby shifting the dynamic of the entire microbial community. Biodegradation begins with the preferential removal of smaller, straight chain alkanes followed by larger straight chain and branched alkanes. Aerobic bacteria break down oil hydrocarbons through a series of oxidation reactions using oxygenases. This produces intermediates that can be integrated into the cell's central metabolic pathways (Fuentes et al., 2014). Large and complex aromatics, resins, and asphaltenes are largely resistant to biodegradation. Although degradation of crude oil hydrocarbons has been shown to occur in the absence of oxygen, aerobic biodegradation is a much faster process than anaerobic biodegradation (Essaid et al., 1995).

Previous investigations into conventional crude oil spills in shallow groundwater environments provide insight into how microbial communities would respond to a dilbit spill (Essaid *et al.*, 2011; National Academies of Sciences, 2016; Rees et al., 2007). Different microbial metabolisms and biodegradation processes dominate within the different redox zones of an oil body (Essaid *et al.*, 2011). Around the edges of the oil body, within the unsaturated zone, saturates and aromatics would be readily oxidized by aerobic heterotrophs. Within the oil body, dilbit's adhesive nature would reduce the surface area available to be attacked by microbes and lead to sediment pore spaces becoming anaerobic (Huang *et al.*, 2019). Below the oil body,

within the saturated zone, aerobic degradation of the contaminant plume would soon deplete any dissolved oxygen rendering the space anoxic shifting the dominant metabolism to anaerobic degradation (Essaid *et al.*, 1995; Essaid *et al.*, 2011) .

Some microbes have the metabolic potential to completely oxidize hydrocarbons to carbon dioxide and water while many others have incomplete biodegradation pathways and instead only partially oxidize the oil components (Mahmoudi et al., 2013b; Yang et al., 2016). While complete mineralization by microorganisms is preferred for post-spill remediation, this is usually not the outcome for large, complex hydrocarbon structures. Instead, the entire microbial community participates in a stepwise transformation of hydrocarbons. In the case of spilled dilbit, microbial uptake is expected to be quite limited, as bitumen represents material that has already undergone degradation (Crosby *et al.*, 2013).

The success of biodegradation as a remediation strategy is highly site specific as it depends on the environmental conditions and the abundance and diversity of microbes that possess the enzymes to break down crude oil constituents (Liao et al., 2015; Liu et al., 2017; Yang *et al.*, 2016). Currently, there are uncertainties surrounding whether the biodegradation potential of dilbit is greater than, less than, or equal to that of conventional crude oil.

1.4. Previous Dilbit Studies

Previous studies investigating the biodegradation of dilbit have predominantly been small-scale laboratory exposures (Deshpande et al., 2018; Hossain et al., 2017; Hua et al., 2018; Huang *et al.*, 2019; Ortmann et al., 2019; Schreiber et al., 2019). However, determining the fate and behavior of dilbit on an ecosystem level is required to ensure that more relevant physical, chemical and biological interactions can be included (Carpenter, 1998; Lee *et al.*, 2015). To address this, there have been several large-scale and in situ studies conducted in recent years, in

both marine and surface freshwater conditions (Cederwall et al., 2020; King et al., 2015; King et al., 2014; Ortmann et al., 2020; Schreiber et al., 2021; Stoyanovich *et al.*, 2019). Of all the studies done to date, only a handful specifically address microbial biodegradation.

Typically, studies have assessed biodegradation by monitoring changes to the concentrations of crude oil hydrocarbon fractions during the exposure period and have linked these changes to shifts in microbial community composition. Using these methods, studies have shown that microbial degradation of dilbit targets mainly the n-alkanes and to a lesser extent small (2-3 ring) PAHs, while biodegradation of large (> 3 rings) PAHs is minimal or non-existent (Cederwall *et al.*, 2020; Deshpande *et al.*, 2018; Ortmann *et al.*, 2019; Schreiber *et al.*, 2019; Schreiber *et al.*, 2021). Potential dilbit-degrading taxa in both marine and freshwater environments, generally, increase in abundance significantly to become major or dominant taxa following exposure. In all studies, the potential dilbit-degrading taxa predominantly belonged to classes *Alphaproteobacteria*, *Gammaproteobacteria*, and *Bacteroidota* and were initially present in very low abundance prior to exposure (Cederwall *et al.*, 2020; Deshpande *et al.*, 2018; Ortmann *et al.*, 2019; Schreiber *et al.*, 2019; Schreiber *et al.*, 2021). The microbial community shows patterns of succession which are hypothesized to reflect changes to the chemical composition of the dilbit as only specific taxa can metabolize the increasingly recalcitrant residue (Deshpande *et al.*, 2018; Schreiber *et al.*, 2019; Schreiber *et al.*, 2021).

1.5. Approaches for Assessing Biodegradation

Employing biodegradation as an oil-spill cleanup strategy requires comprehensive investigations of biodegradation properties. *In situ* characterization methods in particular, are highly relevant as these methods are most likely to yield results that are applicable to developing site-appropriate remediation strategies. Various approaches including use of next generation

sequencing, microbial biomarkers, compound-specific isotope analysis and radiocarbon analysis have been routinely employed in recent studies (Ahad et al., 2010b; Ahad and Pakdel, 2013; Ahad et al., 2018; Atlas et al., 2015; Cowie et al., 2010; Deshpande et al., 2017; Deshpande *et al.*, 2018; Ferguson et al., 2020; Mahmoudi et al., 2013a; Mahmoudi *et al.*, 2013b; Miller et al., 2019; Vázquez et al., 2017).

Microbial community response following an oil contamination event can be monitored using next generation sequencing of 16S ribosomal RNA (rRNA) gene (Caporaso et al., 2012). The 16S rRNA gene codes for the 16S rRNA component of the small subunit of a prokaryotic ribosome and is found in all prokaryotes due to its role in protein synthesis. This gene has nine semi-conserved hypervariable regions (V1-V9) interspersed between highly conserved sequences. Hypervariable regions are targeted and amplified by polymerase chain reaction (PCR) to yield amplified gene fragments called amplicons. These amplicons are then sequenced with next generation sequencing technology (eg. Illumina MiSeq) and results are analysed using bioinformatics to taxonomically classify members of a microbial community (Ahad *et al.*, 2018; Deshpande *et al.*, 2017; Deshpande *et al.*, 2018; Mahmoudi *et al.*, 2013b; Miller *et al.*, 2019; Sun et al., 2015; Vázquez *et al.*, 2017).

In addition to monitoring the taxonomic composition of an impacted microbial community, another key to understanding the biodegradation of petroleum is showing, definitively, that microbes are using petroleum hydrocarbons as a carbon source. Since the organic matter consumed by an organism will be integrated into its cellular components, study of these components in situ can shed light on the nature of the carbon source. Microbial phospholipid fatty acids (PLFAs) are integral components of cell membranes. Because PLFAs are degraded soon after cell death, they are excellent biomarkers for the active microbial

community (Ahad et al., 2010a; Ahad and Pakdel, 2013; Mahmoudi *et al.*, 2013a; Slater et al., 2005).

Simply monitoring crude oil hydrocarbon concentrations has its limitations because hydrocarbon losses cannot be definitively attributed to microbial uptake. Instead, the sources of the carbon metabolized by a microbial community can be accurately identified by studying the natural abundance stable carbon ($\delta^{13}C$) and radiocarbon ($\Delta^{14}C$) isotope compositions of the microbial PLFAs (Ahad *et al.*, 2010a; Slater *et al.*, 2005). PLFAs can be extracted and isolated from contaminated sediment samples. The carbon-isotopic ratios of PLFAs produced by heterotrophic microbes are very similar to the isotopic ratios of potential carbon sources, such as the background total organic carbon (TOC) and the crude oil (Blair et al., 1985; Cowie *et al.*, 2010; Hayes, 2018). $\delta^{13}C$ analysis of individual PLFAs can be used to elucidate carbon sources of specific taxonomic groups within a microbial community. However, $\delta^{13}C$ analysis has limitations, particularly where the $\delta^{13}C$ value of contaminants cannot be resolved from that of background organic material. In such instances, the use of $\Delta^{14}C$ analysis in tandem with $\delta^{13}C$ analysis has proved highly useful (Ahad and Pakdel, 2013; Cowie *et al.*, 2010; Slater *et al.*, 2005). The $\Delta^{14}C$ value of the PLFA indicates the degree to which ^{14}C-depleted substrates, such as diluted bitumen (−1000‰) are being consumed versus more modern TOC (0-200‰; Ahad and Pakdel, 2013; Slater *et al.*, 2005). A very negative $\Delta^{14}C$ PLFA value would therefore provide direct evidence of crude oil biodegradation.

1.6. Objectives

The objectives of this thesis were to address the following two research questions: (1) What is the impact of dilbit on a native soil microbial community? (2) How does dilbit biodegradation compare to that of conventional crude? We achieved this by monitoring the

response of a microbial community to a long-term (104-day) exposure of a dilbit using large-scale soil-filled mesocosms as analogues to natural shallow groundwater systems. Alongside the dilbit treatment, a second exposure treatment of a heavy conventional crude oil was done under identical conditions. This provided a unique opportunity to directly compare the biodegradation potential of both crude oils under controlled conditions and observe changes to the microbial community over time.

CHAPTER 2: Biodegradation of diluted bitumen in shallow groundwater systems

2.1. Introduction

Western Canada has the third largest oil reserves in the world with the majority of those reserves are found in the Alberta oil sands deposit (NRCan, 2020). The oil extracted from this region is a heavily degraded, highly viscous form of petroleum known as bitumen. In order to be transported via pipeline, bitumen is diluted with lighter hydrocarbon fractions (referred to as diluents) to yield a less viscous blend commonly referred to as dilbit (NRCan, 2020; Radović *et al.*, 2018). An estimated 3.9 million barrels per day of dilbit flowed through North American pipelines in 2019, with over 840,000 km of pipeline networks. The risk of inland oil spill is undoubtedly present and there is potential for spills to affect a wide range of freshwater, terrestrial, and groundwater systems (NRCan, 2020). Compared to marine spills, inland spills are in many ways of greater concern as they have a greater potential to occur near populated areas, impact drinking water supplies, and affect environments with a much lower capacity to dilute and disperse the oil (Lee *et al.*, 2015). Soils and shallow groundwater systems, despite being the environment most frequently impacted by pipeline ruptures, have received much less attention compared to marine environments (Owens *et al.*, 1993; Zhao *et al.*, 2021).

Many of the chemical and physical properties of dilbit substantially differ from other commonly transported crude oils leading to unique behavior in the environment. In 2010, dilbit was accidentally released into a tributary creek of the Kalamazoo River in Michigan, causing extensive contamination. Observations from this spill, along with laboratory experiments, showed that dilbit initially floats on the surface of a water body but, during subsequent weathering, changes in its density cause a large portion of dilbit to eventually sink (Dollhopf et

al., 2014; King *et al.*, 2014; McGowan et al., 2012; Radović *et al.*, 2018). As a result, cleanup strategies that were largely developed with conventional crude oils in mind, were less effective when applied to this dilbit spill (Dollhopf *et al.*, 2014; McGowan *et al.*, 2012). Thus, there is an urgent need to understand the key physical and biogeochemical processes that occur during an inland dilbit spill to develop comprehensive remediation strategies.

Biodegradation has been demonstrated to be one of the most cost-effective and least disruptive strategies for containing and removing conventional crude spills from the environment (Hazen et al., 2016; Mahmoudi et al., 2017; Widdel *et al.*, 2010; Yang *et al.*, 2016). The success of this strategy is highly site specific as it depends on both environmental conditions and the abundance and diversity of microbes that possess the enzymes to break down crude oil constituents (Liao *et al.*, 2015; Liu *et al.*, 2017; Yang *et al.*, 2016). Currently, there are uncertainties surrounding whether the biodegradation potential of dilbit is greater than, less than, or equal to that of conventional crude oil. Previous dilbit studies have shown a breakdown of the simplest alkane fractions (Schreiber *et al.*, 2019), while evidence for the degradation of larger aromatic fractions of dilbit has been mixed (Deshpande *et al.*, 2018; Schreiber *et al.*, 2021). In addition, most studies focusing on the biodegradation of dilbit have only considered small-scale short-term (< 30-day) exposures (Davoodi et al., 2020; Deshpande *et al.*, 2017; King *et al.*, 2014; Stoyanovich *et al.*, 2019), which greatly limits our ability to predict the long-term biodegradability of dilbit.

To address these research gaps, we investigated the response of soil microbial communities to a long-term (104-day) exposure of dilbit using large-scale mesocosms as analogues to natural groundwater systems. Alongside the dilbit treatment, a second exposure treatment of a heavy conventional crude oil was done under identical conditions to provide a

unique opportunity to directly compare the biodegradation potential of both oils under controlled conditions. Rather than monitoring changes in petroleum hydrocarbon concentrations, which only provide indirect evidence for biodegradation, we used natural abundance stable carbon ($\delta^{13}C$) and radiocarbon ($\Delta^{14}C$) isotope analysis to provide direct evidence for microbial uptake of dilbit. Natural abundance $\delta^{13}C$ and $\Delta^{14}C$ values of microbial components (e.g. lipids), can be compared to those of the soil organic matter and petroleum hydrocarbons to definitively demonstrate *in situ* biodegradation (Ahad *et al.*, 2010a; Slater *et al.*, 2005). Petroleum products, including dilbit, have no detectable ^{14}C ($\Delta^{14}C$ = -1000‰). This contrasts with surface or near-surface soil organic matter, which has a $\Delta^{14}C$ value that more closely reflects the input of recently fixed carbon (0-200‰; Ahad and Pakdel, 2013; Slater *et al.*, 2005). Thus, the more negative the $\Delta^{14}C$ value of microbial components, the greater the uptake of petroleum-derived carbon by the microbial community. Concurrently, we tracked temporal changes in microbial community composition and diversity using amplicon sequencing of the 16S rRNA genes (Caporaso *et al.*, 2012; Mahmoudi *et al.*, 2013b) to identify key dilbit-degrading taxa.

Our results showed strong evidence for microbial uptake and degradation of both dilbit and conventional crude oil based on $\Delta^{14}C$ value of microbial lipids. Amplicon sequencing revealed shifts in microbial communities in response to dilbit exposure and suggest that *Polaromonas*, a known hydrocarbon-degrading bacterial genus, is a key dilbit-degrading taxon. This study provides the first direct evidence of continuous dilbit biodegradation by a soil microbial community and represents one of the longest duration dilbit biodegradation experiments to have been carried out thus far.

2.2. Materials and Methods

2.2.1. Mesocosm Construction

In July 2019, approximately 2000kg of vadose zone soil was collected from the Gault Nature Reserve. This reserve, located approximately 40 km east of Montreal, Quebec, Canada, encompasses one of the largest remaining sections of primary forest remaining in the St Lawrence River Valley (McGill University, 2022). Following collection, the soil was immediately transported to the Laboratoires pour l'innovation scientifique et technologique de l'environnement (LISTE) facilities of the Institut national de la recherche scientifique (INRS) in Québec City, Québec. There, soil was sieved through a 2 cm mesh and mechanically rotated in 100 L high density polyethylene barrels until homogenized before being weighed and determining water content (5.38 ± 0.02%). Homogenized soil was then evenly distributed between three mesocosms which were each composed of a stainless-steel mesocosm (60 cm width x 100 cm height) lined with polytetrafluoroethylene (PTFE; Figure 4). Within each mesocosm, 312.80 ± 0.20 kg of soil (dry mass) was compacted to a height of 70 cm using a jack drill. Seven 1 cm diameter outflow ports in the bottom of each mesocosm directed leachate water into seven 1 L amber glass bottles resting below. Ports were fitted with PTFE pipe fittings with fibreglass wicks threaded through them. To limit evaporation these ports were sealed to the leachate collection bottles with PTFE thread tape (Thermo Fisher Scientific, Waltham, USA). Wicks were in contact with the bottom layer of soil in the mesocosm and, relative to the sandy soil, had a net negative capillary pressure which helped to draw the leachate from the mesocosm to maintain unsaturated conditions (Everett and McMillion, 1985).

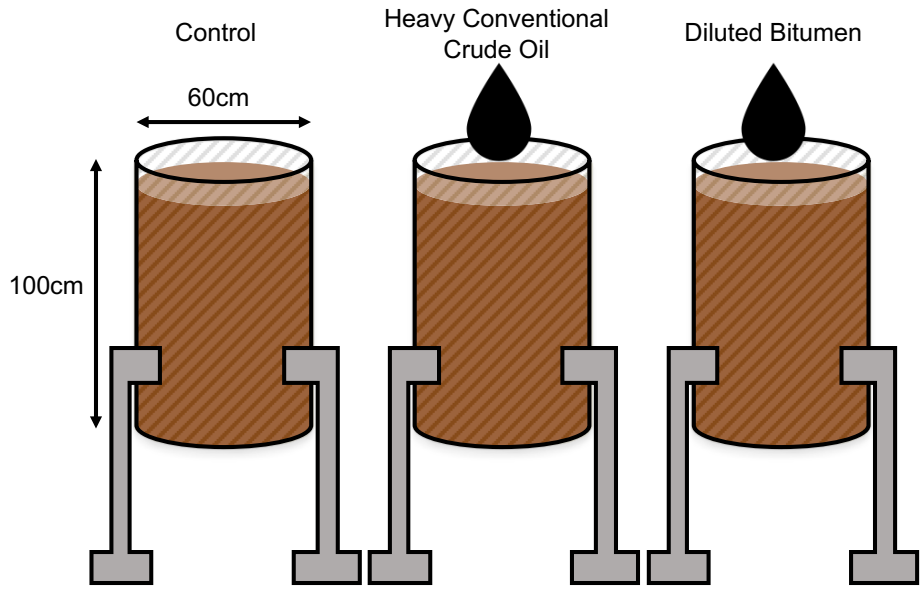

Figure 4. Diagram of large mesocosm experimental set-up.

2.2.2. Experimental Conditions

The mesocosms were designed to be representative of vadose soil systems in the Greater Montréal Area during spring and fall recharge. These seasons were selected as they allow for plenty of groundwater infiltration without interference from the high rates of evapotranspiration that occur in the summer, or from the snow and ice cover seen in the winter (Lewis et al., 2009). The mesocosms were maintained in a temperature-controlled room at 10°C. Artificial rainwater to simulate local precipitation acidity (pH 4.8; Keresztesi et al., 2020; Koehler and Wassenaar, 2010; Vet et al., 2014) was made up using a 3:2 (vol/vol) stock solution of sulfuric:nitric acid and added to each mesocosm twice a week for a total of 6.25 L of water per week. On August 2nd, 2019 (Day 0), conventional heavy crude oil and diluted bitumen (dilbit) were distributed on the surface of the mesocosms. The heavy conventional crude (CC) mesocosms received 1.86 kg of heavy conventional crude oil while the dilbit (DB) mescocosm, received 1.89 kg of Cold Lake blend. Both samples originated from transmission pipelines: Cold Lake blend refers to bitumen

produced by in situ extraction in the Cold Lake region of Alberta, while the conventional heavy crude refers to various Western Canada Sedimentary Basin crude oils with similar physical and chemical properties. The proportions of saturates, aromatics, resins and asphaltenes in the oils determined gravimetrically following silica gel chromatography were 25.4, 51.9, 9.5 and 13.2% and 30.4, 45.8, 8.5 and 14.2% in the DB and CC samples, respectively. The third mesocosm was left unamended as a control. The experiment concluded 104 days later

2.2.3. Soil Sample Collection

Soil cores were collected using a stainless-steel soil core sampler (AMS, American Falls, ID, USA) affixed with a slide hammer and a removable 15.2 cm (length) x 3.8 cm (diameter) aluminum cylinder. The core sampler and removable cylinder were rinsed with acetone and distilled water between mesocosms. The first core was collected immediately prior to the addition of the crude oil treatments to characterize the initial soil conditions on what is referred to as Day 0. Coring was done on a weekly basis for the first month (Day 0, Day 6, Day 13, and Day 20) and then on a biweekly basis for the remainder of the experiment (Day 34, Day 48, Day 62, Day 76, Day 90, and Day 104) with 10 cores collected in total (Figure 5). Each core consisted of three core sections corresponding to three depths in the soil profile: 0-15.2 cm, 15.2-30.5cm and 30.5-45.7 cm (Table S1, Figure 5). Soil from each soil core section was subdivided with the majority placed into a combusted (450 °C for 4 hours) 500 mL glass jar to be used for PLFA extractions and ~10 mL placed into a sterile 50 mL polypropylene tube with a high-density polyethylene cap (VWR International, Mississauga, ON, Canada) to be used for DNA extraction. All soil samples were stored at -20°C until extractions took place.

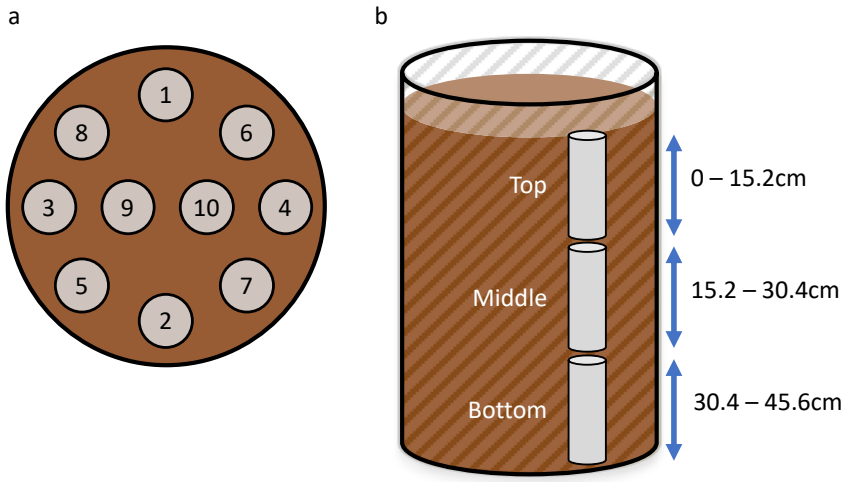

Figure 5. Diagram showing the spatial arrangement of soil cores (shown in grey) collected from mesocosms as seen from above (a) and from the side (b). Ten soil cores were collected from each mesocosm over the exposure period and each core was divided into three sub-sections (top, middle and bottom).

To minimise the hydraulic disturbance caused by repeated coring, core holes were filled in with a 1:1 mixture of sodium bentonite clay tablets (Volclay® PureGold™ 3/8 inch, CETCO, Bethlehem, PA, USA) and powder (Envrioplug Grout, Wyo-Ben Inc., Billings, USA) following the collection of each core. This material expanded when mixed with water so that the soil remained compact and at the same time still allowed water to permeate vertically. Both bentonite pellets and powder were certified by the National Sanitation Foundation International standard and American National Standard for drinking water additives (NSF International, 2016).

2.2.4. Microbial Lipid Extraction and Analysis

Phospholipid fatty acids (PLFAs) are essential membrane lipids of microbial cells and biomarkers for the active microbial population. PLFAs were extracted from soil cores collected from the mesocosms following the modified Bligh and Dyer method (White et al., 1979) employed by Ahad *et al.* (2018). Throughout the extraction process, efforts were made to

minimize potential contamination. Glassware was thoroughly cleaned and combusted (450 °C for 4 hours). Glass syringes with polytetrafluoroethylene (PTFE)-tipped plungers, PTFE caps and stopcocks, and metal scoops in contact with samples were solvent rinsed beforehand, typically with methanol (MeOH) and dichloromethane (DCM). During temporary storage, samples were reduced to a small volume under ultrahigh purity N2 and kept in the freezer at -20 °C.

Frozen sediment cores samples were thawed to room temperature then around 50 g of soil from each of the six samples was weighed out into 250 mL glass jars. Approximately 100 mL of a MeOH, DCM, and phosphate buffer solution (2:1:0.8, v/v) was added to create a soil-solvent mixture. Following 10 minutes of sonication at 25 ℃, the supernatant containing the lipid fraction, was decanted into a separate 250 mL glass jar. The process was repeated using 60mL of the 2:1:0.8 MeOH:DCM:phosphate buffer solution. Soil particles and some oil residue were removed from the decanted solution by filtering with solvent-rinsed glass microfibre filters (VWR International, 1.5 μm particle retention) into separatory funnels.

Organic and aqueous phases were separated by pouring filtered sediment extract into a separatory funnel along with 20 mL of ultra-pure water and 1-2 g combusted NaCl to improve separation. The separatory funnel was inverted and agitated until it appeared homogenous and then allowed to separate for about 10-15 minutes at which point there was a clear delineation between the two phases. The denser organic phase (DCM) containing the fatty acids was drained and collected. The aqueous layer was retained in the separatory funnel for two additional extractions with 20 mL of DCM. Sample volume was then reduced to approximately 5 mL by rotary evaporation.

The organic phase was separated by gravity mesocosm chromatography using three solvents: DCM, acetone, and MeOH to yield fractions containing non-polar lipids (F1); neutral

lipids (F2); and polar lipids, including phospholipids, (F3). The stationary phase was prepared using a slurry of combusted (450 °C for 4 h) fully activated silica gel (70-230 mesh, Silicycle, Québec, Canada) in hexane. The silica gel was then added to a 30 cm (length) × 2 cm (diameter) glass mesocosm to a height of 8 cm along with a small quantity (several grams) of anhydrous sodium sulphate to remove residual water. The sample was added to the mesocosm and eluted with 60 mL of each solvent. Eluant from all three fractions were collected and reduced to a small volume using a rotary evaporator. F1 and F2 were archived while PLFA-containing F3 was transferred to 12 mL glass vials and evaporated to dryness with ultrahigh purity N2.

The PLFAs were converted to fatty acid methyl esters (FAMEs) by mild alkaline methanolysis (adapted from Guckert et al., 1985). The dried lipid sample was redissolved in 1.0 mL of a toluene:isotopically characterized MeOH (1:1, v/v) and 1.0 mL of isotopically characterized methanolic KOH (the methylation agent). The mixture was then vortexed and incubated for 1 hour at 37°C. Once cooled to room temperature, samples were neutralized (pH between 6 and 7) by 200 µL 1N Acetic Acid and phase separated into an upper organic layer and lower aqueous layer with 2 mL of hexane:DCM (4:1, v/v), 2.0 mL of nano-pure water and ~0.5 g of combusted NaCl. The organic layer containing the FAMEs was extracted a total of three times with two subsequent additions of 2 mL of hexane:DCM (4:1, v/v). The FAMEs-containing phase was transferred to a 12 mL vial and reduced to a small volume under ultrahigh purity N2.

A secondary silica gel chromatography cleanup was done to eliminate impurities in samples prior to analysis. Short glass mesocosms (i.e., combusted 5” Pasteur pipettes) were filled halfway with combusted fully activated silica gel in a hexane slurry as described above. Three fractions were collected using 4 mL of the following solvents: 4:1 hexane:DCM, DCM, and MeOH. Fractions from each sample were eluted into separate 4 mL glass vials. The 4:1

hexane:DCM and MeOH fractions were archived in the -20°C freezer. The DCM fraction containing the purified FAMEs was reduced to 1.0 mL under ultrahigh purity N2 and transferred to a 2 mL amber glass vial.

The FAMEs samples were analysed using an Agilent (Santa Clara, CA, USA) 7890A/5975C TAD Series gas chromatography – mass spectrometer (GC-MS) equipped with a Zebron ZB-5HT mesocosm (30 m; 0.25 mm i.d.; 0.25 μm film) at the Delta-Lab of the Geological Survey of Canada (GSC-Québec). The following GC oven temperature program was used: 40 °C (1 min), 20 °C/min to 130 °C, 4 °C/min to 160 °C, 8 °C/min to 300 °C (5 min) as per Ahad *et al.* (2018).

PLFAs were identified by comparing the mass fragmentation patterns and retention time to a bacterial reference standard (Bacterial Acid Methyl Esters CP Mix, Sigma-Aldrich, Oakville, ON, Canada). PLFAs were identified as Z:nΔx, where Z is the total number of carbon atoms on the fatty acid chain, n is the number of double bonds and Δx indicates the location of the double bond if known. The letters A, B, and C denote different isomers whose double bond position is unknown. Cyclopropyl PLFAs are denoted with the prefix “cyc”. Methyl group branching is denoted by the prefixes “i” for the iso-isomer, “a” for the anteiso-isomer, and “br” if the position of the methyl group is unknown (branched isomers are differentiated by letters A, B, and C).

Quantification was done using external FAME standards (12:0, 14:0, 16:0, 18:0, and 20:0). Calibration curves and quantitation methods were set up using MSD ChemStation Data Analysis software (Agilent). The distributions of individual PLFAs in each sample are reported here as a mole percentage (mol %) relative abundance.

2.2.5. $\delta^{13}C$ Analysis of Microbial Lipids

The stable carbon isotope content ($\delta^{13}C$) of individual PLFAs was determined using a gas chromatography – isotope ratio mass spectrometer (GC-IRMS) at the Delta-Lab of the Geological Survey of Canada. The system consisted of a TRACE 1310 GC with a HP-5 mesocosm (60m; 0.32mm i.d.; 0.25 μm film) paired with a Delta V IRMS via a GC IsoLink (Thermo Fisher Scientific, Bremen, Germany). The IsoLink combustion reactor was maintained at 1050 ℃. The GC oven temperature program was the same as that previously outlined above for GC-MS analysis.

An external standard mixture containing 5-α-androstane ($\delta^{13}C$= −31.35‰), obtained from the Biogeochemical Laboratories at Indiana University, and five in-house FAME isotopic standards (12:0, 14:0, 16:0, 18:0, and 20:0; $\delta^{13}C$ = −28.8‰, −29.5‰, −30.4‰, −23.8‰ and −28.0‰ respectively) was injected into the GC-IRMS after every six sample injections to assess accuracy. Samples were run in duplicate and peaks were manually integrated using Isodat software (Thermo Fisher) to obtain $\delta^{13}C$ ratios for specific PLFAs. All $\delta^{13}C_{PLFA}$ values were corrected for the isotopically characterized methyl group added to each FAME during mild alkaline methanolysis by the following equation:

$$\delta^{13}C_{PLFA} = [\delta^{13}C_{measured} - (f_{MeOH} \times \delta^{13}C_{MeOH})]/1\text{-}f_{MeOH} \qquad (1)$$

where fMeOH is the fraction of C atoms derived from MeOH. The $\delta^{13}C_{MeOH}$ value was -51.3‰.

2.2.6. $\delta^{13}C$ Analysis of Total Organic Carbon (TOC)

Soils were freeze-dried and 2-3mg of each sample were transferred to a 40 μL rigid silver capsule (IVA-Analysentechnik e.K.). Using a pipet, 30 μL of distilled water was added into each capsule. Samples were acidified followed by adding 10 μL of 8% sulphurous acid to each capusle. Samples were then placed in drying oven at 60 degrees for approximately 1h until dry.

Samples were acidified a second time with 30 μL of 8% sulphurous acid and dried as before. The acidification and drying process was repeated using 50 μL of 8% sulphurous acid until no effervescence was noticed in the sample capsule. The capsules were then sealed with pliers, folded into a spherical shape, and placed into a tin capsule to improve combustion in the elemental analyser (EA). The $\delta^{13}C$ values of total organic carbon (TOC) in soil were measured by EA-IRMS. High sand content contributed to a greater inconsistency associated with weighing out the small sample masses required for TOC analyses and thus a higher variability in $\delta^{13}C$ values.

2.2.7. $\Delta^{14}C$ Analysis of Microbial Lipids and Total Organic Carbon (TOC)

The masses of recovered PLFAs were too low for compound-specific radiocarbon analysis; consequently, ^{14}C contents were determined in the bulk PLFA fractions. In some cases, samples from multiple depths were combined to meet mass requirements for bulk ^{14}C analyses. FAMEs dissolved in DCM were transferred by syringe into a 40 μL rigid silver capsule (IVA-Analysentechnik e.K.), dried in an oven at 50°C for 30 min, and sealed with pliers following a protocol similar to that previously used for preparation of organic extracts for ^{14}C analysis (Ahad et al., 2020; Ahad et al., 2021). Samples were placed in quartz tubes with CuO oxidizer, sealed under vacuum, and combusted to CO_2 at 900°C. CO_2 was then reduced to graphite and measured for its $^{14}C/^{12}C$ ratio using a 500 kV compact accelerator mass spectrometer (AMS) unit (National Electrostatics Corporation, Middleton, WI, USA) at the W.M. Keck Carbon Cycle AMS facility at UC Irvine. Ratios were then corrected with the ratio of Oxalic Acid I (SRM 4990) and normalized for ^{13}C fractionation to be presented in the standard $\Delta^{14}C$ notation (Stuiver and Polach, 1977).

The $\Delta^{14}C$ values of total organic carbon (TOC) in soil were also determined by using a the AMS unit (National Electrostatics Corporation, Middleton, WI, USA) at the W.M. Keck Carbon Cycle AMS facility at UC Irvine. To prepare TOC samples, soil samples were freeze-dried before being sent to the AMS facility. There, TOC samples were decalcified with 1N HCl at 70°C, washed with ultrapure MilliQ water and dried prior to combustion to CO2. $\Delta^{14}C$ values were then determined using the same methodology as was used for the PLFAs, described above. To assess the accuracy and precision of $\Delta^{14}C$ analyses, both modern (butter FAMEs) and fossil (Ordovician shale aromatic hydrocarbons) standards of similar masses to those of samples were prepared in the same manner as described above. Based on replicate analyses of these standards, the error incorporating both accuracy and precision for $\Delta^{14}C$ analyses was < 20‰.

All $\Delta^{14}C_{PLFA}$ values were corrected for the isotopically characterized methyl group added to each FAME during mild alkaline methanolysis by the following equation:

$$\Delta^{14}C_{MeOH} = [\Delta^{14}C_{measured} - (f_{MeOH} \times \Delta^{14}C_{MeOH})]/1\text{-}f_{MeOH} \qquad (2)$$

Where f is the mol % weighted average of the fraction of C atoms derived from MeOH on each FAME. The $\times \Delta^{14}C_{MeOH}$ value was - 998.2‰.

Contributions of potential carbon sources to ^{14}C content of bulk PLFA fractions were estimated using a two end-member mass balance:

$$\Delta^{14}C_{PLFA} = (1 - f_{soil}) \times \Delta^{14}C_{petroleum} + f_{soil} \times \Delta^{14}C_{soil} \qquad (3)$$

where $\Delta^{14}C_{PLFA}$ corresponds to the isotopic signature of the PLFAs, fsoil is the fraction of carbon contributed by the background soil TOC, 1- fsoil is the fraction of carbon contributed by petroleum, $\Delta^{14}C_{petroleum}$ is isotopic signature of DB or CC and $\Delta^{14}C_{soil}$ is isotopic signature the background soil TOC.

2.2.8. Statistical Analyses of PLFA Data

All statistical analyses and visualizations were done in R, version 4.0.2 (R Core Team, 2020). Normality and homogeneity of variance of PLFA mol % and PLFA $\delta^{13}C$ value datasets were evaluated with the Shapiro-Wilk test ($P<0.5$) and the Levene's test ($P<0.5$), respectively. For both datasets, the assumptions of normality and equal variance required for analysis of variance (ANOVA) tests were not met. As an alternative to ANOVA, the non-parametric Kruskal-Wallis test followed by a Dunn's multiple comparison test with Holm adjustment was done to reveal if significant differences existed between metadata groups (treatment type/sample depth/sample day) in these datasets. Calculations were done using the rstatix package (Kassambara, 2021).

To explore the variability of the mol % of the main PLFAs between metadata groups, principal component analysis (PCA) was performed for each depth separately. Biplots of the first two principal components (PCs) were produced using ggplot2 (Wickham, 2011) and used to visualize the dissimilarity among the PLFA distributions of the microbial communities. Loading scores for individual PLFAs were included on the biplots to show the relative contribution of each PLFA to the PC axes.

2.2.9. DNA Extraction and Sequencing of 16S rRNA Genes

Genomic DNA was extracted from 45 soil cores, in replicate, using the DNeasy PowerSoil DNA extraction kit from Qiagen (Hilden, Germany) following the manufacturer's protocol. DNA extracts were submitted to the Ronholm Lab (McGill University) for library preparation and high-throughput 2 x 250 bp paired-end sequencing of bacterial 16S V4 rRNA genes using an Illumina MiSeq (San Diego, CA, USA). Data were processed using Quantitative Insights Into Microbial Ecology 2 (QIIME2) v2021.2 (Bolyen et al., 2019). Demultiplexed,

primer free sequences were imported into QIIME2 command line interface (q2cli). Sequence quality was visually assessed with the q2-demux plugin. Denoising was done using the DADA2 pipeline (Callahan et al., 2016) implemented with the q2-dada2 plugin. This corrected amplicon sequencing errors, filtered out chimera and singleton reads, merged paired end reads, and produced an amplicon sequence variant (ASV) table. To optimize merging of forward and reverse reads, reads were trimmed at the position where median Phred quality scores dropped off lower than 30. Forward and reverse reads were truncated at nucleotide positions 250 and 162 respectively. This reduced the total read count from 6,382,607 to 3,812,693 with an average of 39,715 counts per sample. A q2-feature-classifier classify-sklearn Naïve-Bayes taxonomy classifier trained for 99% accuracy on SILVA v138 (Quast et al., 2012) was implemented via the q2-feature-classifier plugin to assign taxonomy to the representative sequences of the ASVs. It should be noted that SILVA v138 implements the Genome Taxonomy Database taxonomy system, which reclassifies the class *Betaproteobacteria* as an order within the class *Gammaproteobacteria* (Parks et al., 2018). The align-to-tree-mafft-fasttree pipeline via the q2-phylogeny plugin included both the ASV alignment using MAFFT (Katoh et al., 2002) and the construction of the phylogenetic tree from the aligned sequences using fasttree (Price et al., 2010). Files generated in the QIIME2 pipeline were then exported for use in downstream statistical analyses.

2.2.10. Statistical Analyses of Amplicon Data

All statistical analyses and visualizations were done in R, version 4.0.2 (R Core Team, 2020). ASV counts were rarefied (subsampled without replacement) to 4162 which equated to the number of reads for the smallest sample using the phyloseq R package (McMurdie and Holmes, 2013). Beta diversity metrics were calculated using Weighted UniFrac distance with

phyloseq. Results of the distance matrix were visualized by principle coordinate analysis (PCoA) using the phyloseq and ggplot2 R packages (Wickham, 2011). Differences in microbial community composition between metadata groups (treatment type/sample depth/sample day) were assessed using permutational multivariate analysis of variance (PERMANOVA). The homogeneity of within-group dispersions was assessed by permutation multivariate analysis of dispersion (PERMDISP). Both PERMANOVA and PERMDISP were implemented using the vegan R package (Oksanen et al., 2013).

Normality and homogeneity of variance of the relative abundance of individual taxonomic groups were evaluated with the Shapiro-Wilk test ($P<0.5$) and the Levene's test ($P<0.5$), respectively. For all datasets, the assumptions of normality and equal variance required for analysis of variance (ANOVA) tests were not met. As an alternative to ANOVA, the non-parametric Kruskal-Wallis test followed by a Dunn's multiple comparison test with Holm adjustment was done to reveal if significant differences existed between metadata groups (treatment type/sample depth/sample day) in these datasets. These calculations were done using the rstatix package (Kassambara, 2021).

2.3. Results

2.3.1. PLFA Identification and Quantification

The total concentrations of PLFAs extracted from individual samples varied widely over the course of the exposure (Figure 6) but did not show any trends across sampling time, depth or treatments. Total PLFA concentrations ranged from 8.18 to 37.57 ng/g soil which is attributable to variability in grain size from sample to sample. Overall PLFA distributions (as mol %) for the most abundant compounds were similar across all samples (Figure 7). The most abundant PLFAs across all DB, CC and control samples were 16:0 (17.0 – 23.0%) and 18:1B (10.4 –

16.2%). Other abundant PLFAs (> 3% average mol %) included cyc17:0 (5.00 – 9.46%), 16:1Δ9 (5.30 – 7.70%), 19:1A (5.68 – 8.30%), i−15:0 (3.82 – 7.60%), 18:1A (3.61 – 6.20%), a−15:0 (3.23 – 5.39%), br17:0A (3.50 – 4.35%), 16:1B (3.43 – 4.46%), and 18:2Δ9,12 (2.56 – 4.47%). Similar PLFA distributions were observed in microbial communities involved in biodegradation of petroleum hydrocarbons (Ahad *et al.*, 2010a; Ahad and Pakdel, 2013). In all treatments, 16:0, a general bacterial biomarker, and 18:1B, a biomarker for gram-negative bacteria, showed a slight increase in abundance over the exposure period (Figure 7). The gram-positive bacterial biomarkers, i−15:0 and a−15:0, both decreased for DB and CC treatments. In contrast, cyc17:0, a biomarker for gram-negative bacteria and petroleum-degrading bacteria, only increased in CC and DB treatments (Figure 7).

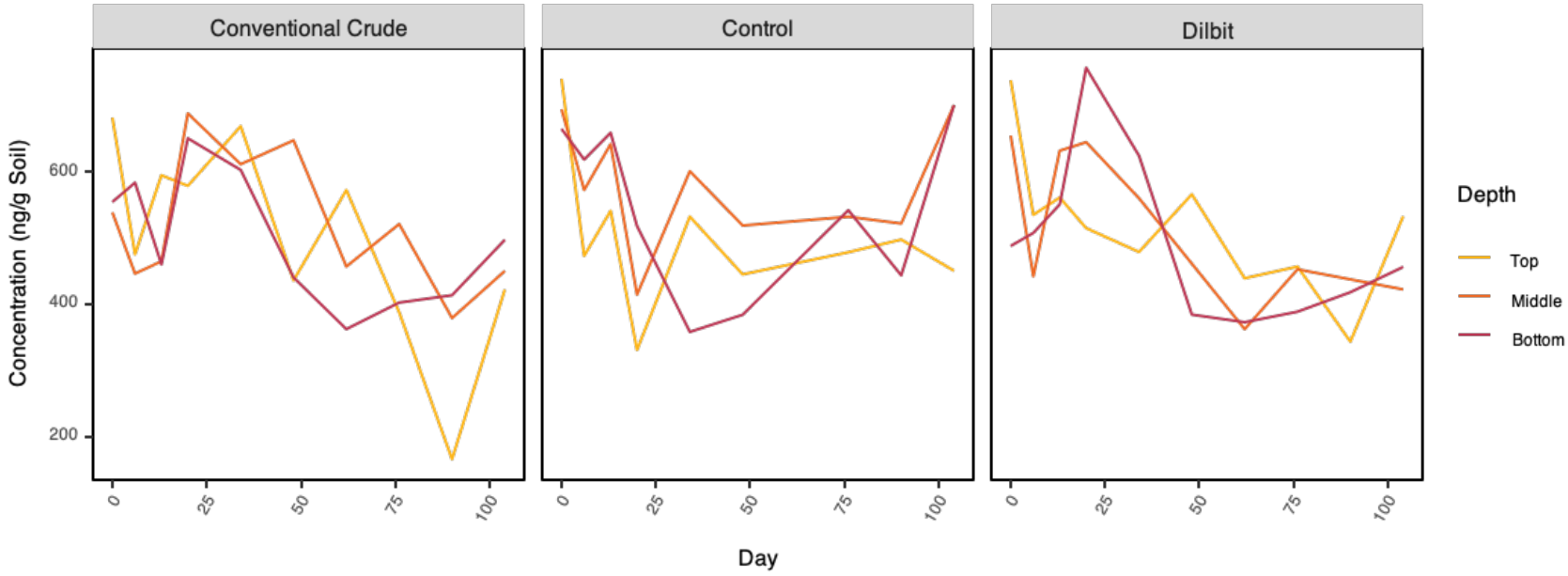

Figure 6. Total PLFA concentrations (ng/g soil) from top, middle, and bottom depths of conventional crude, control and dilbit treatments over the 104-day exposure period.

Principle component analysis (PCA) was performed on mol % data for the main PLFAs from each depth separately. PCA biplots show a progressive change in PLFA distributions occurred over time in oil-affected samples and in the controls (Figure 8). The first axis explained 55.03%, 46.47%, and 49.75% of the variation in the top, middle, and bottom depths respectively. Separation of samples on PC1 axis depended on duration of treatment with PLFA distributions of early stage (day 6-48) CC and DB samples clustered more closely with controls while late-stage (day 48-104) CC and DB samples clustered separately. PC1 had positive loadings of cy17:0, 16:0, 16:1 and 18:1B and negative loadings of i−15:0 and 18:1A in all three depths. Greater mol % in 16:0, 18:1B, and cyc17:0 were associated with late-stage DB and CC samples while greater mol % in i−15:0 and 18:1A were associated with control and early-stage DB and CC samples.

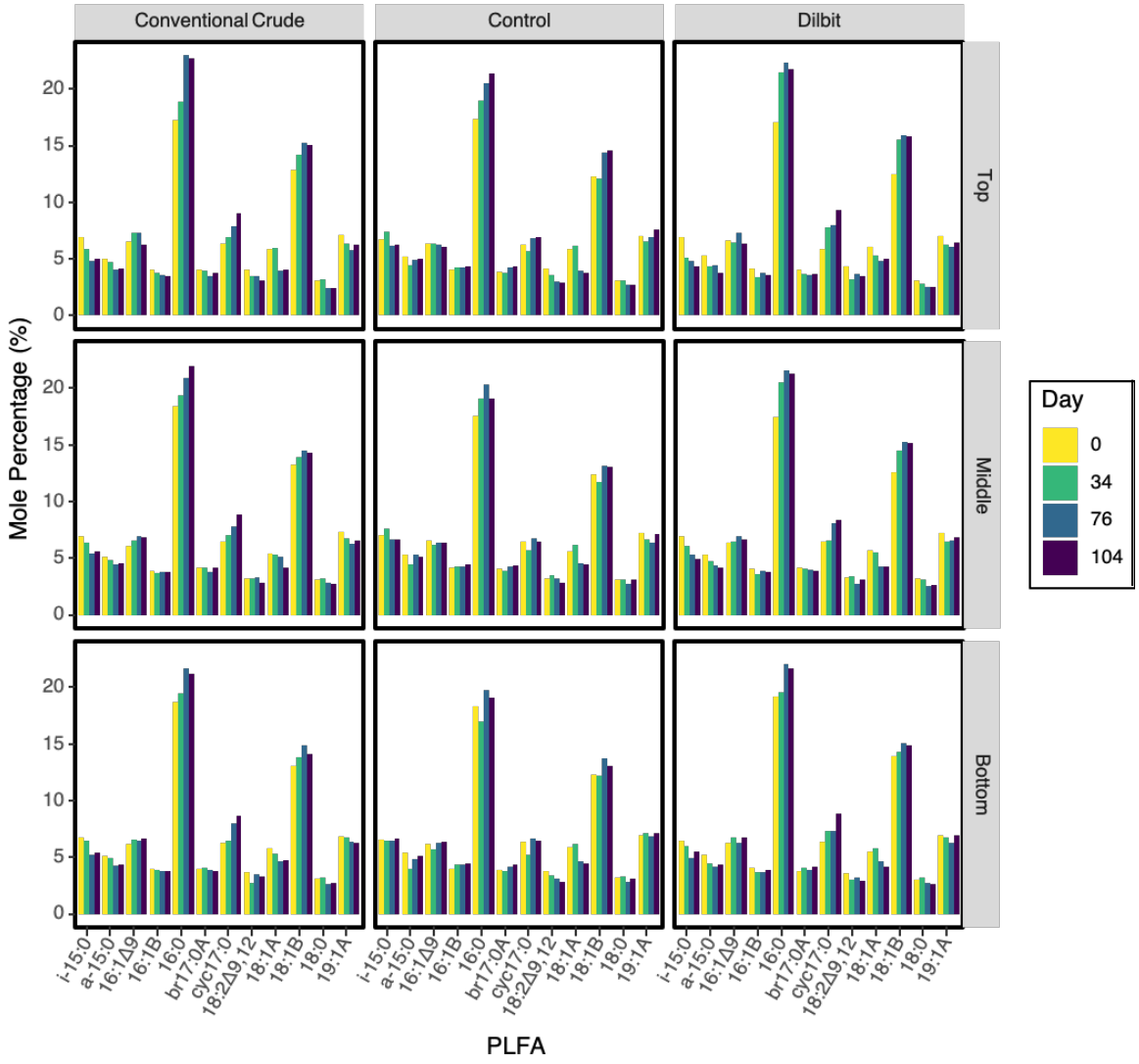

Figure 7. Relative abundance distributions (mole percentage) of 12 of the most abundant PLFAs in samples collected from the top, middle and bottom depths of conventional crude, control, and dilbit treatments during the 104-day exposure period.

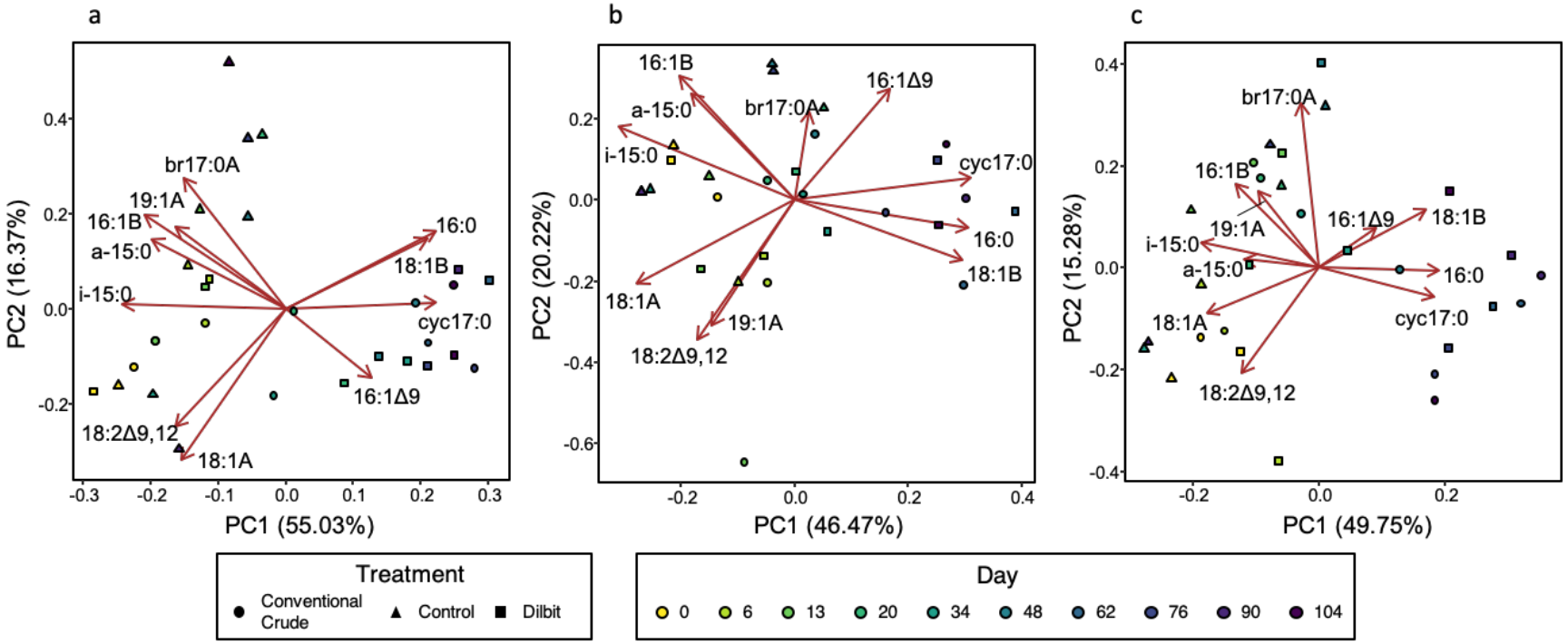

Figure 8. Principal component analysis (PCA) biplot of the relative abundance (mol %) of PLFAs for a) top, b) middle and, c) bottom depths. Arrows represent scaled loadings of each PLFA, indication their contribution to creating the component.

2.3.2. Compound-Specific $\delta^{13}C$ Values of Individual PLFAs

It was not possible to fully resolve certain PLFAs on the GC-IRMS. As a result, several PLFAs were integrated together to obtain $\delta^{13}C$ values for a PLFA group; 16:1Δ9 and 16:1B were grouped as well as 18:2Δ9,12; 18:1A, and 18:1B. The $\delta^{13}C$ values of individual or grouped PLFAs ranged from -30.5‰ to -24.0‰ (Figure 9). The most enriched PLFA was a−15:0, with an average $\delta^{13}C$ value from all three mesocosms (DB, CC and Control) of -25.2 ± 0.5‰ over the entire length of the experiment. The most depleted PLFA was 19:1A, with an average $\delta^{13}C$ value of -29.0 ± 0.7‰. The $\delta^{13}C$ of the TOC in the control soil was -27.3 ± 0.3‰ (n=6, % TOC = 1.7) while dilbit and conventional crude oil had values of −29.9‰ and −29.3‰ respectively. There were statistically significant differences in $\delta^{13}C$ values of cyc17:0 ($P<0.05$) and the combined PFLAs 16:1Δ9 and 16:1B ($P<0.05$) between treatment types. The $\delta^{13}C$ values of cyc17:0 were significantly more depleted in both CC and DB compared to the control ($P<0.5$). The combined 16:1Δ9 and 16:1B group was significantly more depleted in ^{13}C in CC compared to the control ($P<0.5$). In general, the $\delta^{13}C$ values of individual PLFAs showed no clear trends between depths or over time.

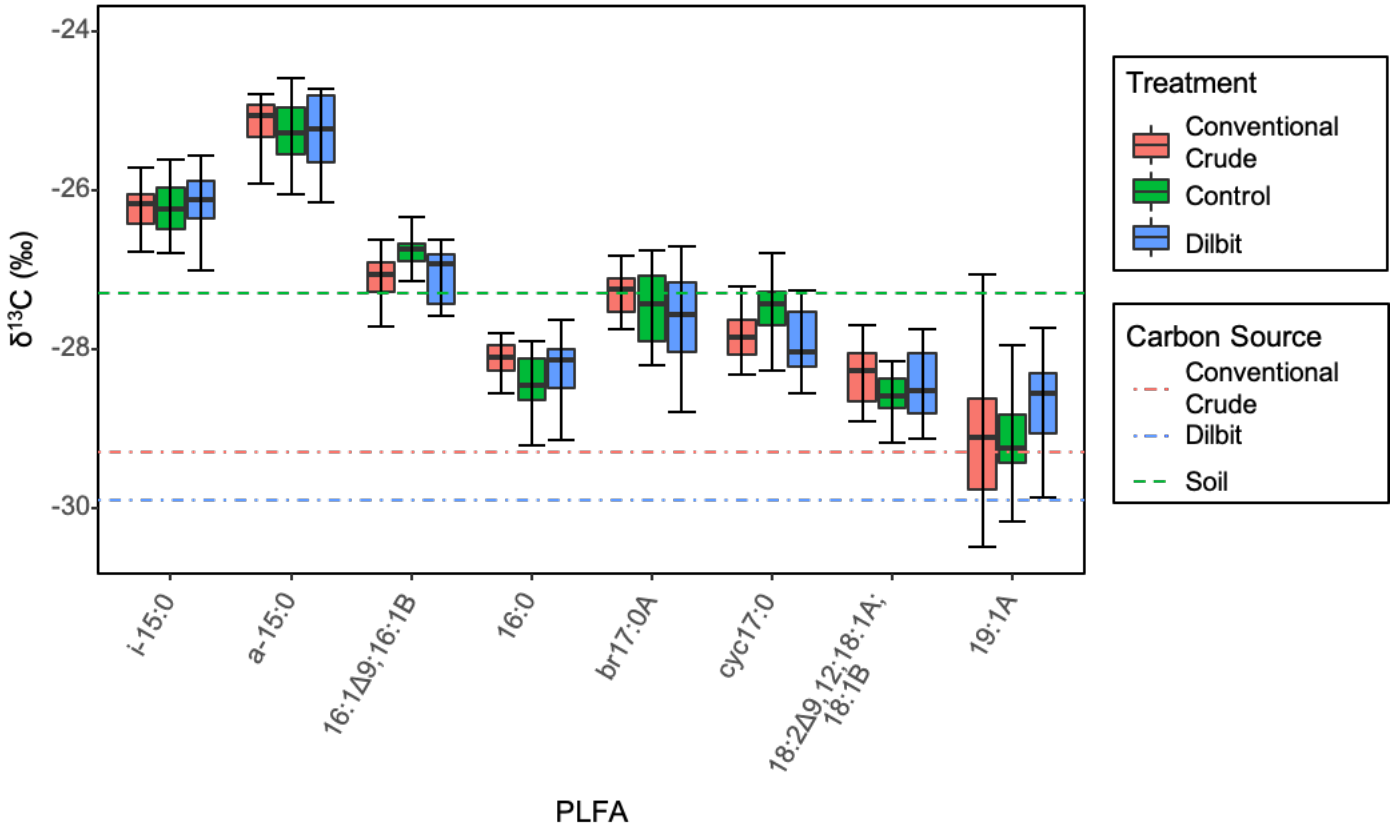

Figure 9. Boxplot of the corrected $\delta^{13}C$ values of the main PLFAs for all samples over the course of the 104-day experiment. Error bars represent standard deviations between samples. Outlier points are not shown but were included in calculations. The horizontal lines denote the $\delta^{13}C$ values of the potential carbon sources (soil TOC, conventional crude and dilbit).

2.3.3. $\Delta^{14}C$ Values of Bulk PLFAs

Bulk PLFA ^{14}C contents for DB and CC were assessed from individual top, middle, and bottom depths on Days 34 and 62 and from combined depths on Day 104. The control bulk PLFA ^{14}C contents were determined from combined depths on Days 0 and 104 (Figure 10). $\Delta^{14}C$ values of TOC in the control from combined depths was measured on Days 0 and 104.

Over the exposure period, the average $\Delta^{14}C$ values decreased for both CC and DB treatments, pointing to microbial uptake of crude oil throughout the 104-day exposure. Fossil fuels like DB and CC are completely depleted in ^{14}C and thus have a $\Delta^{14}C$ value of −1000‰, while modern organic matter contains recently photosynthetically fixed CO_2 and is ^{14}C-enriched (Δ14C≈+55‰, Turnbull et al., 2007). The $\Delta^{14}C$ of bulk PLFAs ranged from −221.1‰ to −54.7‰ in the DB treatment and from −259.4‰ to −107.1‰ in the CC treatment. The $\Delta^{14}C$ of bulk PLFAs in the control at middle, bottom and combined depths ranged from 0.3 to 53.7‰. However, the $\Delta^{14}C$ values in the top depths of the control were much more depleted with day 34 and day 62 values at −28.5‰ and −46.1‰ respectively. There was also a decrease observed in $\Delta^{14}C$ values in TOC from −22.6‰ to −46.8‰ between days 0 and 104. This discrepancy can be attributed to the release of volatile compounds from neighbouring DB and CC mesocosms contaminating the surface of the control mesocosm. Overall, the $\Delta^{14}C$ of bulk PLFAs in the control were even more enriched in ^{14}C relative to the bulk soil TOC (−34.7‰). This indicates that microbes were preferentially degrading the more modern and ostensibly labile constituents within the background soil TOC, a finding observed in previous studies (Cowie *et al.*, 2010; Kramer and Gleixner, 2008). These results provide strong evidence that microbial degradation and uptake of both DB and CC hydrocarbons occurred during the 104-day incubation.

Using two end-member mass balance (Eq. 3), we calculated the relative contribution of carbon sources to the ^{14}C content of the PLFAs in the DB and CC samples (Table S2). In soils impacted by DB, between 2.9 and 20.1% of carbon was derived from fossil carbon. In soils impacted by CC, between 7.3 and 24.0% of carbon was derived from fossil carbon. Thus, while there was certainly uptake of DB and CC, the background soil organic matter remained the dominant carbon source for microbial communities.

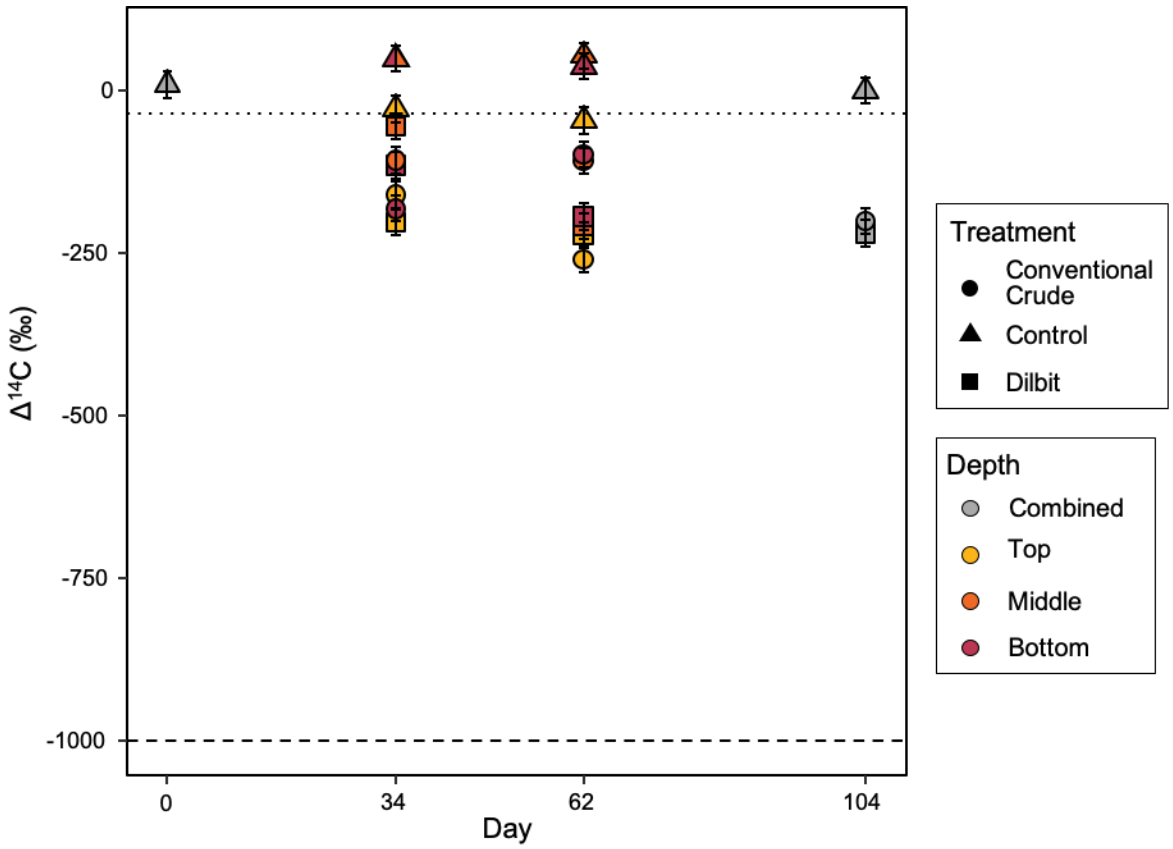

Figure 10. The $\Delta^{14}C$-PLFA values of samples. Top, middle and bottom depths were combined for Days 0 and 104 Control as well as Day 104 dilbit and heavy conventional crude samples. Top, middle, and bottom depths were analysed individually for Days 34 and 64 samples. The dotted line represents the $\Delta^{14}C$ value of the soil TOC (−35‰) while the dashed line represents the $\Delta^{14}C$ value of dilbit and heavy conventional crude (−1000‰). Error bars represent ± 20‰ accuracy and precision of $\Delta^{14}C$ measurements.

2.3.4. Microbial Community Composition

Sequencing of 16S amplicons yielded a total of 6,382,607 reads across 90 samples. Following quality control, the total read count was reduced to 3,812,693 with an average of 39,715 reads per sample. The total number of amplicon sequence variants (ASVs) present in the filtered dataset was 26,641. The overwhelming majority of ASVs (17736) were assigned to Bacteria and only 69 were assigned to Archaea. The dominant bacterial phylum across all samples was *Proteobacteria*, making up 32.7 – 60.1% of ASVs across all samples. Other abundant phyla (> 1% average abundance) included *Actinobacteriota* (8.48 – 21.4%), *Acidobacteriota* (6.75 – 17.0%), *Chloroflexi* (2.57 – 9.66%), *Bacteroidota* (1.71– 19.8%), *Myxococcota* (0.77 – 7.81%), *Verrucomicrobiota* (1.20 – 6.90%), *Planctomycetota* (0.82 – 5.91%), *Gemmatimonadota* (1.25 – 3.72%), and *Firmicutes* (0.43 – 5.96%) (Figure 11). All major phyla were less in abundant, on average, in the DB and CC exposures than in the control with the exception of *Proteobacteria* ($P < 0.001$), whose relative abundance significantly increased over time ($P < 0.001$).

There were significant differences in the relative abundances of several phyla between depths for all treatments ($P < 0.05$). In the control, *Acidobacteriota*, *Verrucomicrobiota*, and *Myxococcota* had a significantly higher relative abundance in the top depth than the middle and bottom depths over the exposure period. Meanwhile *Actinobacteriota* and *Firmicutes* were significantly less abundant in the top depth than the middle and bottom depths. In DB, *Verrucomicrobiota* was significantly more abundant in the top depth than the middle depth over the exposure period. *Firmicutes* and *Myxococcota* were significantly more abundant in the top depth than in both the middle and bottom depths. *Chloroflexi* was more abundant in the middle

depth than the top and bottom depths over the exposure period. No significant differences between depths were detected for CC.

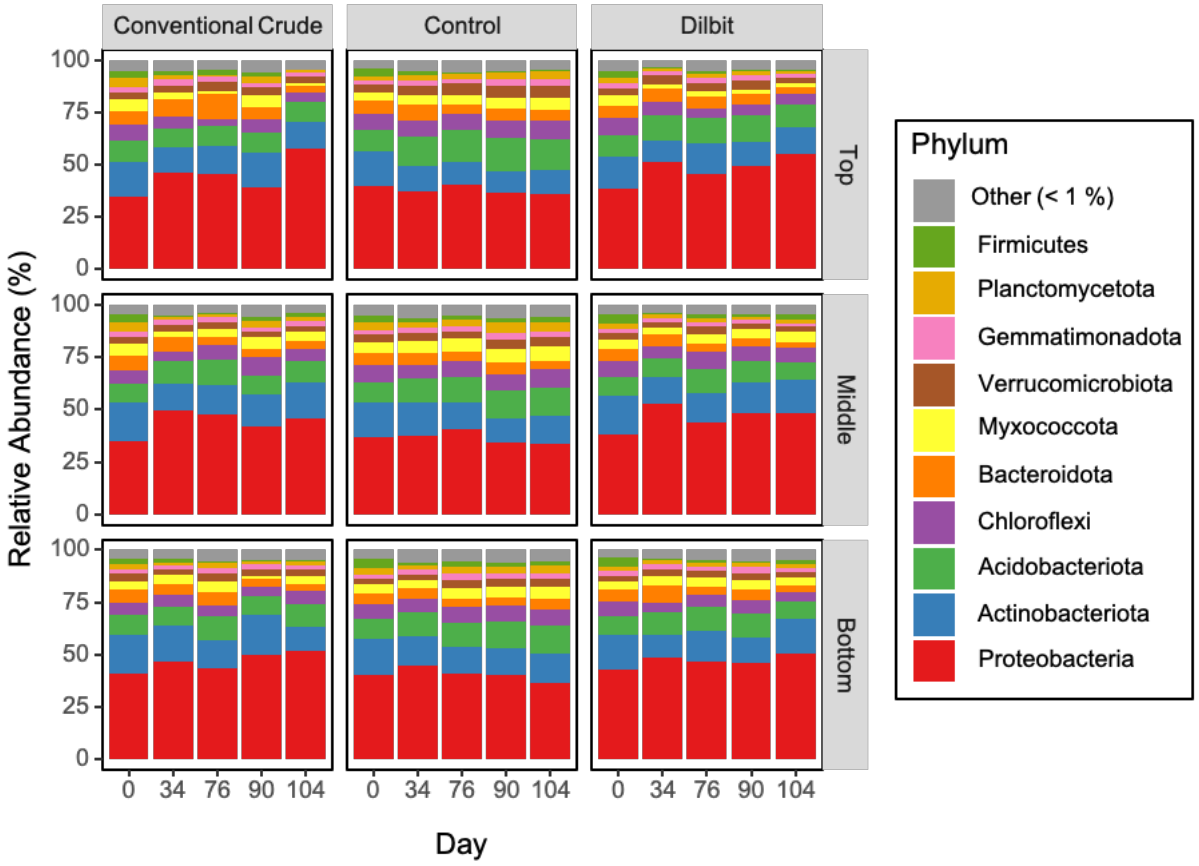

Figure 11. Microbial community composition at the phylum level. The relative abundances in the sequences are expressed as a percent (%). Facets group mesocosm treatments (top x-axis), and depths (y-axis). Phyla with an average relative abundance less than 1% are collectively labelled as Other.

Gammaproteobacteria was the dominant class (Figure 12) and showed significant differences in relative abundances between control and DB treatments and between control and CC treatments ($P < 0.05$). The average relative abundance of *Gammaproteobacteria* in all three mesocosms at Day 0 was 16.8 – 26.3%. During the exposure period, the relative abundance of *Gammaproteobacteria* increased significantly to 23.7 – 37.0% and 21.0 – 44.3% in the DB and CC treatments, respectively ($P < 0.05$). In contrast, the relative abundance of

Gammaproteobacteria remained at 18.1 – 27.6% in the control treatment. *Actinobacteria* were also significantly more abundant in CC (7.52 – 18.0%) and DB (7.71 – 13.2%) as compared to the control (5.48 – 11.3%) ($P < 0.05$). The average relative abundance of *Alphaproteobacteria* was significantly greater in DB (14.8 – 22.9%) than in both CC (13.8 – 22.8%) and the control (14.3 – 20.4%) during the exposure period. There was no significant difference in the relative abundance of *Alphaproteobacteria* between CC and control ($P < 0.05$).

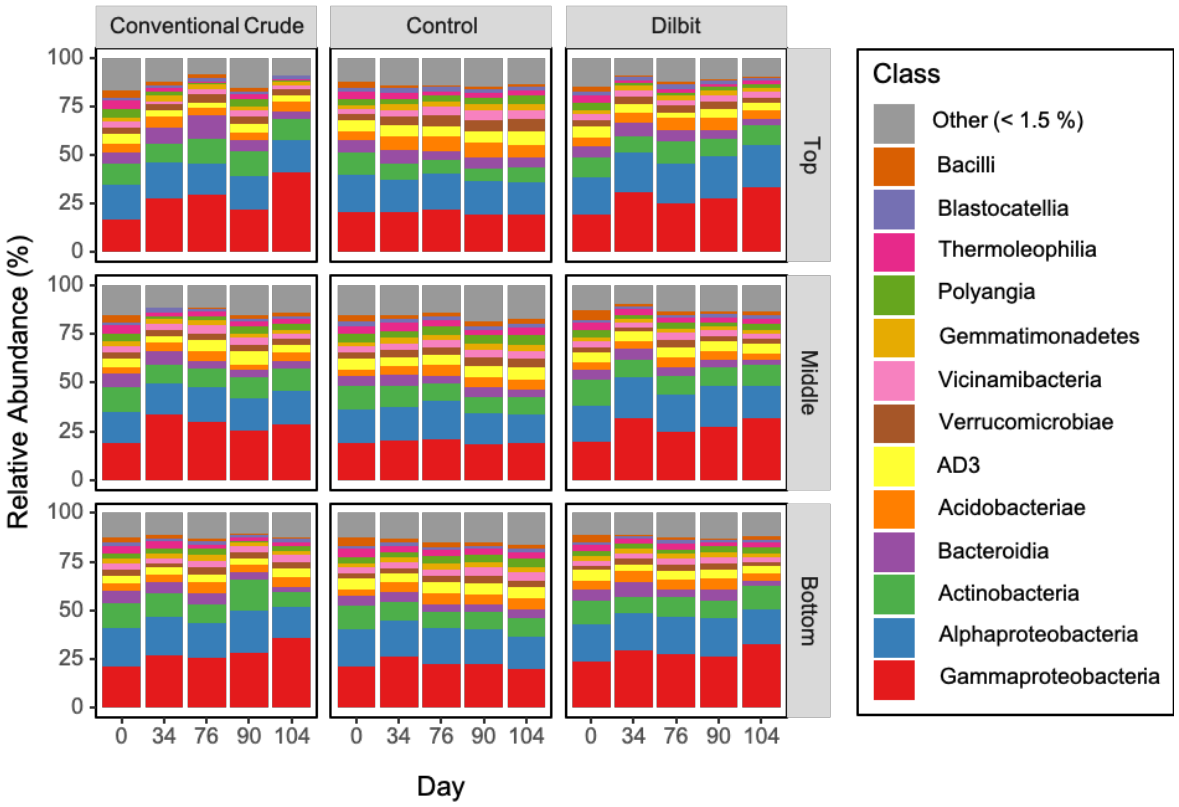

Figure 12. Microbial community composition at the class level. The relative abundances in the sequences are expressed as a percent (%). Facets group mesocosm treatments (top x-axis), and depths (y-axis). Phyla with an average relative abundance less than 1% are collectively labelled as Other.

The top depth again grouped separately from the middle and bottom depths for both DB and the control ($P < 0.05$). In the control, *Verrucomicrobiae* and *Acidobacteriae* were more abundant at the top depth than the middle and bottom depths. There were no significant differences between the middle and bottom depths in the control. In DB, *Alphaproteobacteria* was more abundant in the top depth compared to the bottom while *Verrucomicrobiae* and *Acidobacteriae* were in greater abundance in the top relative to the middle. In both DB and control the relative abundances of *Bacili*, *Thermoleophilia*, and *Polyangia* were lower in the top depth than in the middle and bottom depths.

Within *Gammaproteobacteria*, the dominant order was *Burkholderiales* whose relative abundance significantly increased from an average of 12.3 – 16.9% on Day 0 to 17.4 – 32.2% and 14.6 – 35.2% in DB and CC treatments ($P < 0.05$). *Corynebacteriales* (*Actinobacteria*), *Sphingomonadales* (*Alphaproteobacteria*), and *Caulobacterales* (*Alphaproteobacteria*) all had significantly greater relative abundance in DB and CC than in the control. There was also a significantly greater relative abundance of *Sphingomonadales* in DB than in CC. In CC, *Micrococcales* (*Actinobacteria*) was more abundant than in the control ($P < 0.05$) (Figure 13).

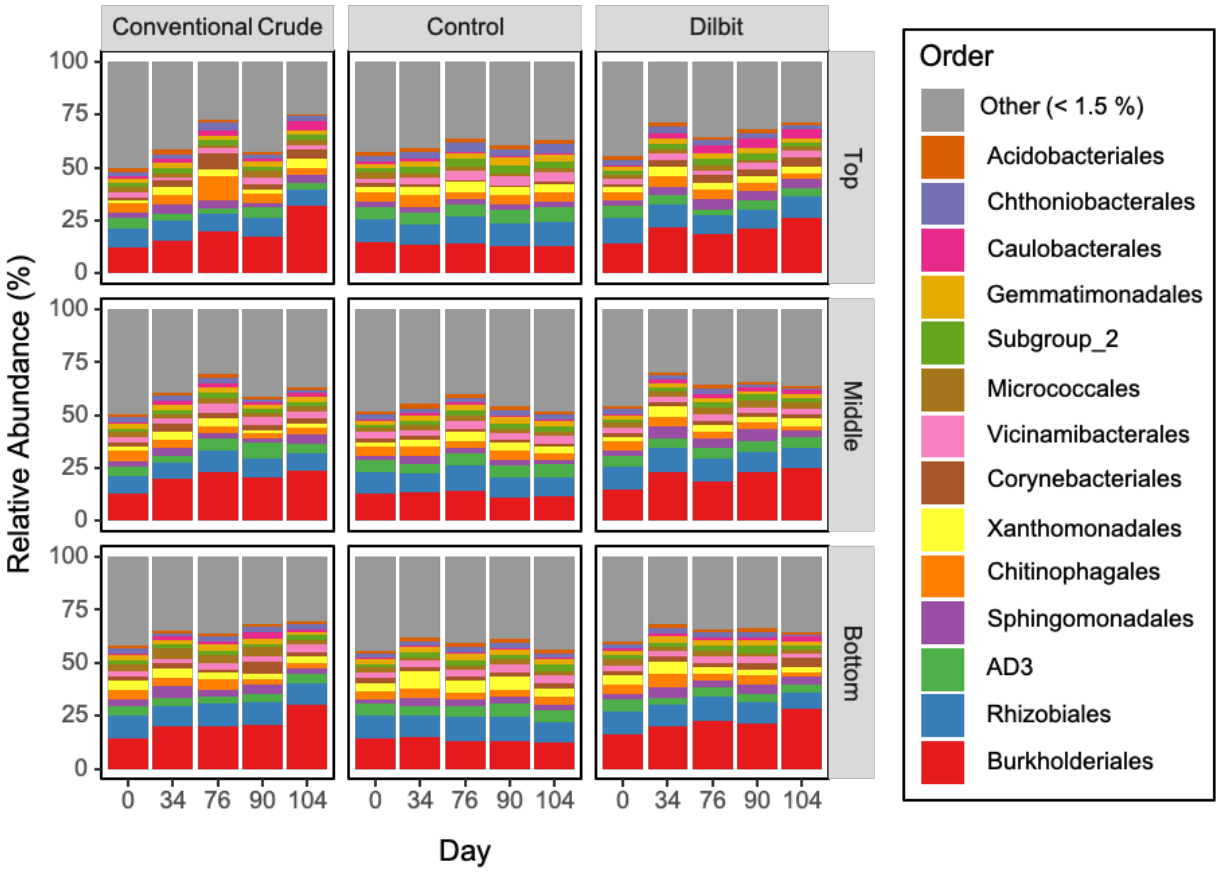

Figure 13. Microbial community composition at the order level. The relative abundances in the sequences are expressed as a percent (%). Facets group mesocosm treatments (top x-axis), and depths (y-axis). Orders with an average relative abundance less than 1.5% are collectively labelled as Other.

At the genus level, dramatic increases in relative abundances of *Polaromonas* from within the order *Burkholderiales* were observed over time (Figure 14). At day 0, *Polaromonas* accounted for <1% of sequences but by day 104 it comprised 8.9 – 18.2% across all depths of DB-impacted soils and 8.0 – 17.2% across all depths of CC-impacted soils while remaining at <1% for the control. There were also significantly higher proportions of *Phenylobacterium*, *Mycobacterium*, and an unknown genus from the family *Comamonadaceae* (the same family as *Polaromonas*) in DB and CC relative to the control ($P < 0.05$).

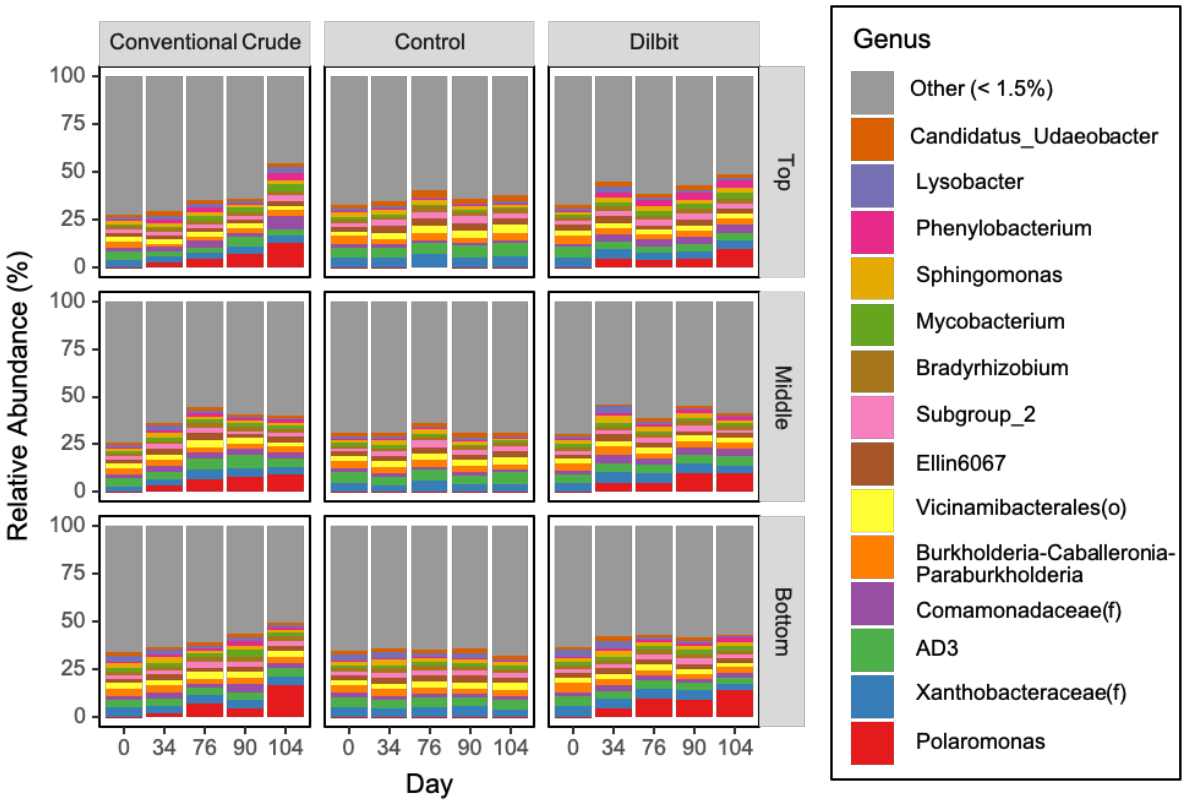

Figure 14. Microbial community composition at the genus level. The relative abundances in the sequences are expressed as a percent (%). Facets group mesocosm treatments (top x-axis), and depths (y-axis). Genera with an average relative abundance less than 1.5% are collectively labelled as Other.

Changes in microbial community structure over time were visualized for each sampling depth (top, middle and bottom) using Principal Coordinate Analysis (PCoA) of weighted unifrac distances based on the relative abundance of ASVs (Figure 15). For all depths, unaffected samples (day 0 and controls) clustered separately from oil-affected samples within the ordination space, indicating that the addition of oil led to changes in the microbial community composition. For all three depths, visual inspection of PCoA plots showed that controls clustered separately from DB and CC treatments while the two oil treatments largely overlapped with each other.

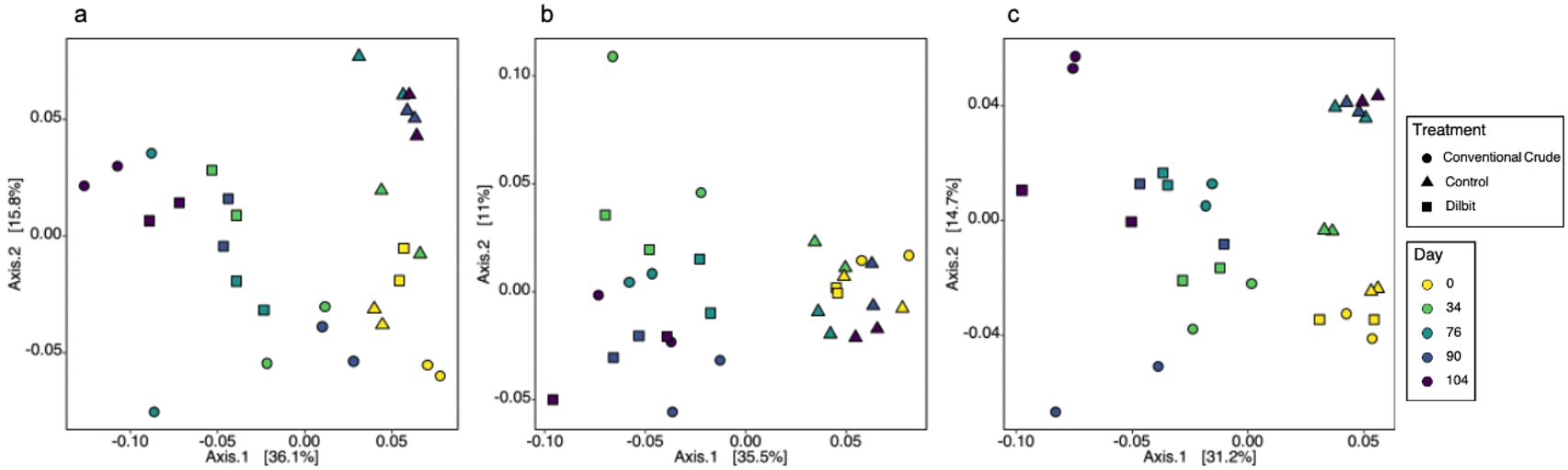

Figure 15. Principal coordinate analysis (PCoA) of samples taken from the a) Top, b) Middle, and c) Bottom depths, based on Weighted-Unifrac distances. Treatment and sampling day are represented by coloured symbols according to the legend. Sample replicates are shown with the same symbol.

Statistical significance of the differences in microbial community composition were assessed using permutational multivariate analysis of variance (PERMANOVA) which requires within-group dispersions to be homogenous. CC-treated samples displayed much greater dispersion than DB treated samples. Permutation multivariate analysis of dispersion (PERMDISP) found that the dispersions between treatment groups were not homogenous ($P<0.05$) in the top depth and that the CC treated samples had more compositional variance than control and DB samples. Therefore, it is uncertain whether any differences detected by PERMANOVA at this depth were attributable to differences in the community composition between groups or differences in the compositional variance between groups.

PERMANOVA tests were conducted on samples at each depth. For top, middle and bottom depths, CC and DB treatments were significantly different from the control but not from each other ($P<0.05$). This suggests that microbial communities were strongly affected by the presence of oil but there were no detectable differences in response between the CC and DB treatments. PERMANOVA test were also conducted for each treatment. The results showed significant differences between depths in DB and the control but not CC. The microbial communities at the top depth of the control and DB, were significantly different than those at the middle and bottom depths ($P<0.05$). For CC, the top depth was found to have a significantly greater dispersion than the middle and bottom depths (PERMDISP with TukeyHSD post hoc, $P<0.05$). Despite not having homogenous dispersion, no significant differences in community composition between depths in CC were found.

Although there were differences found between DB and CC in terms of the relative abundance of certain taxa, the overall community structures of the two treatments were largely similar. PCoA and PERMANOVA tests found no significant difference between the microbial

communities affected by DB and CC but did clearly differentiate them from Day 0 and control communities. However, DB and CC did show different in terms of their dispersion with microbial communities in CC being more variable than in DB and the control over time and between depths. Based on the DNA results we concluded that DB and CC had significant impacts on the microbial community and exposure to the two oil types yielded similar microbial responses.

2.4. Discussion

The main objectives of this study were to gain insight into the biodegradation potential of dilbit relative to a conventional crude oil and to identify potential dilbit-degrading microbes present in a shallow groundwater system. We achieved this by running side-by-side simulated spills of dilbit and conventional heavy crude oil in mesocosms that were representative of natural shallow groundwater systems. We measured the stable carbon and radiocarbon isotopic contents of PLFAs to look for evidence of microbial uptake of petroleum-hydrocarbons and we employed 16S rRNA amplicon sequencing to observe changes to the diversity and composition of the microbial community over time.

The distributions of PLFAs in DB, CC, and control treatments showed slight changes over the course of the experiment. The increase in the mol % cyc17:0, 16:0, 18:1B, and 16:1Δ9, and decrease in a−15:0, and i−15:0 were associated with microbial communities exposed to CC and DB and were indicative that shifts in community composition did occur. Cyc17:0, 18:1B, and 16:1Δ9 are biomarkers for gram-negative bacteria (Wilkinson and Ratledge, 1988). Previous studies have reported similar increases in the abundance of gram-negative PLFA biomarkers following exposure to oil treatments (Bastida et al., 2016; Green and Scow, 2000; Li et al., 2018; Margesin et al., 2007). In addition to being a biomarker for gram-negative bacteria, cyc17:0 has

been associated with petroleum degrading microbial communities in numerous studies (Ahad *et al.*, 2018; Cowie *et al.*, 2010; Greenwood et al., 2009). This increase in gram-negative was confirmed by the amplicon sequencing data.

The amplicon sequencing data showed that the gram-negative bacterial phylum, *Proteobacteria*, dominated the microbial community and their relative abundance increased over the exposure period in DB and CC mesocosms. *Proteobacteria* is known to include a multitude of hydrocarbon-degrading bacteria that have been shown to contribute to crude oil degradation (Ahad *et al.*, 2018; Bastida *et al.*, 2016; Deshpande *et al.*, 2018; Hazen *et al.*, 2016; Mahmoudi *et al.*, 2013b). The dominant DB and CC-degrader identified in our study was *Polaromonas*, a genus within the order *Burkholderiales*. In addition to *Polaromonas*, there were several other genera that significantly increased in abundance during the DB and CC exposure. These included *Phenylobacterium*, *Mycobacterium*, and an unknown genus from the family *Comamonadaceae* all of which are known oil-degrading bacteria (Atlas *et al.*, 2015; Kweon et al., 2011; Rodgers-Vieira et al., 2015; Yang *et al.*, 2016). Previous genomic analyses have shown that numerous bacteria within the taxa Burkholderiales, including *Polaromonas*, have the metabolic potential to degrade a broad spectrum of aromatics as it possesses the genes used in many peripheral and central ring-cleavage pathways (Hanson et al., 2012; Jeon et al., 2003; Pérez-Pantoja et al., 2012). In addition, *Polaromonas* was identified as a potential dilbit-degrader in a recent study where dilbit biodegradation by bacterial enrichments in freshwater microcosms was monitored over 72-days (Deshpande *et al.*, 2018). Deshpande *et al.* (2018) found that *Polaromonas*, along with other bacterial genera, began to increase as concentrations of larger aromatic and branched alkane fractions began to decrease. In their study, *Polaromonas* reached its highest abundance on day 40 and day 72. In our exposure, *Polaromonas* reached its highest relative abundance

more than three months following the spill, on day 104. We speculate that this slow, but consistent, increase indicates that *Polaromonas* was metabolizing the larger, more complex hydrocarbon fractions that did not undergo immediate weathering.

Hydrocarbon metabolism by bacteria under aerobic conditions results in PLFAs with $\delta^{13}C$ values that closely mirror those of the carbon source (typically PLFAs are depleted by < 3‰) (Ahad and Pakdel, 2013; Cowie *et al.*, 2010; Hayes, 2001). The observation that all $\delta^{13}C$ PLFA values were within 3‰ of the potential carbon sources thus reflects the oxic conditions in soil mesocosms and aerobic biodegradation of DB of heavy CC (Figure 9). The depleted $\delta^{13}C$ values of cyc17:0 and the combined 16:1Δ9 and 16:1B in DB and CC relative to the control pointed to uptake of ^{13}C-depleted oil relative to more ^{13}C-enriched soil TOC. Both PLFAs are biomarkers for gram-negative bacteria and have also been associated with oil-degrading microbial communities (Ahad *et al.*, 2018; Greenwood *et al.*, 2009). Interestingly, *Polaromonas* strains have been shown to predominantly feature 16:1Δ9 and cyc17:0 in their PLFA profiles (Kämpfer et al., 2006; Sizova and Panikov, 2007). The enriched $\delta^{13}C$ values of i−15:0 and a−15:0 suggest ^{13}C-enriched fractions of the background soil TOC were the carbon source rather than the ^{13}C-depleted oil. This, along with the decrease in mol % of i−15:0 and a−15:0 following exposure to DB and CC implied that i−15:0 and a−15:0 are biomarkers for microbes negatively impacted by oil. There were no discernable trends in $\delta^{13}C$ values over time or between depths, likely due to the small difference between the $\delta^{13}C$ of TOC and DB, CC (2.0 and 2.6‰ respectively), relative to the margin of error in $\delta^{13}C$ measurements (±0.5‰).

Changes in the ^{14}C content of bulk PLFAs over the exposure period lent further support to the evidence for biodegradation of DB and CC. Relatively depleted $\Delta^{14}C$ values on Days 34, 62, and 104 compared to the control revealed that microbes in oil-affected soils were

assimilating DB and CC throughout the exposure (Figure 10). While DB and CC uptake did occur, soil organic carbon remained the main carbon source for the microbial community. In soils impacted by DB, between 2.9 – 20.1% of carbon was derived from fossil carbon. In soils impacted by CC, between 8.3 – 24.0% of carbon was derived from fossil carbon. This preferential uptake of relatively ^{14}C-enriched background soil TOC at petroleum-contaminated sites has been observed in several other studies. Ahad et al. characterized the carbon sources utilized by the active microbial communities in shallow groundwater systems underlying three petroleum service stations. They found that that higher petroleum concentrations and lower soil TOC levels corresponded to greater utilization of fossil carbon up to 43% (Ahad *et al.*, 2010a). Mahmoudi et al., collected PLFAs from soils surrounding an industrial site that historically used PAHs. Maximum contributions of PAH-derived carbon to microbial PLFAs were found to range from 12 to 71% but microbial utilization of carbon sourced from more modern organic matter predominated (Mahmoudi *et al.*, 2013a).

There were some discrepancies in the $\Delta^{14}C$ values in the control, with the PLFAs in top depths of the control being much more depleted than middle and bottom depths (Figure 10). There was also a decrease in the $\Delta^{14}C$ values of TOC in the control (combined depths) from −22.6‰ to −46.8‰ between days 0 and 104. This inconsistency can be attributed to the release of volatile compounds from the neighbouring DB and CC mesocosms contaminating the top depth of the control. This would have led to uptake of ^{14}C-depleted hydrocarbons by microbes in the top depth of the control. This theory is supported by the trends seen in the amplicon sequencing results. During the exposure period, microbial community composition in the top depth of the control was significantly different that in the middle and bottom depths ($P<0.05$). In

addition, the microbial community in the control on day 0 was found to be significantly different from all other days of the exposure ($P<0.05$).

Over a 104-day exposure period using large-scale mesocosms, this study is the first to provide direct evidence of continuous microbial uptake of dilbit in a shallow subsurface environment. Similarities in the microbial response to DB and CC spills demonstrated that, in shallow groundwater systems, the biodegradation potential of these two oils is equal. Data generated by this study can be used inform the development of effective DB spill-response strategies, specifically the potential for biodegradation by natural soil microbial communities to act as a remediation strategy.

CHAPTER 3: Implications and Future Research

3.1. Conclusions

The long-term biodegradation of two crude oil products, dilbit and conventional heavy crude oil, by a natural microbial community were assessed using large-scale soil mesocosms. These mesocosms were intended to be representative of shallow groundwater systems. Evidence of biodegradation was found by employing a combination of DNA, PLFA, and natural abundance isotopic analyses. PLFA profiles showed increases to the relative abundance (mol %) of gram-negative bacterial biomarkers known to be associated with petroleum-degrading populations. The $\delta^{13}C$ values of gram-negative bacterial biomarkers were depleted in CC and DB samples, suggesting uptake of both crude oil types by gram-negative bacteria. Continuous DB and CC uptake were directly confirmed by bulk PLFA $\Delta^{14}C$ values however, soil TOC remained the dominant carbon source for the microbial community. The oil-degrading gram-negative bacterial genus, *Polaromonas,* identified using 16S rRNA amplicon sequencing, dominated the communities of DB- and CC-impacted soils. The top depths of all three mesocosms differed from middle and bottom depths in terms of microbial community composition and isotopic values, highlighting that the effects of DB and CC were not uniform across soil depths. The similarities in PLFA profiles, isotopic content, and microbial community composition led us to conclude that the long-term biodegradation potential of DB and CC in shallow groundwater systems were similar.

3.2. Future Research

While we attempted to replicate natural shallow groundwater systems a logical next step for this research would be to move from laboratory-based studies to *in situ* mesocosms to incorporate more environmentally relevant conditions. A large-scale *in situ* mesocosm study

would provide potentially more representative insights into dilbit biodegradation. It would be interesting to see if field data shows the same trends as laboratory-based experiments to get a better idea of the limitations of this mesocosm study. In addition, it is important to capture a range of geographical locations and seasonal conditions as factors such as soil type and temperature, affect not only the behaviour of dilbit but also the diversity and composition of the native microbial community (Hamamura et al., 2006). This would shed light on whether or not microbial response to dilbit contamination is consistent across a range of shallow groundwater environments.

The 104-day exposure period in our study represents one of the longest-term dilbit biodegradation studies conducted to date. However, our results indicate that biodegradation likely continues beyond this timeframe. Future work could also look at scaling up this simulated spill experiment on both a physical and temporal scale. While this could provide greater insight on the long-term biodegradation potential of dilbit, mesocosms have certain limitations and drawbacks that may be amplified with a lengthened exposure period (Schindler, 1998). These would have to be considered in the experimental design of future studies.

3.3. Research Implications

Production and transportation of dilbit, and other unconventional crude oils, are expected to increase in coming decades (CAPP, 2020). The possibility of a dilbit spill is therefore a reality that presents a risk to a wide range of freshwater, terrestrial, and groundwater systems (NRCan, 2020). Relative to conventional crude oil, information on the fate and behavior of diluted bitumen spills in the environment is limited. Most research to date has focused on short-term biodegradation in marine and freshwater settings. Compared to marine spills, inland spills are in many ways of greater concern as they have a greater potential to occur near populated

areas, affect drinking water supplies, and affect environments with a much lower capacity to dilute and disperse the oil (Lee *et al.*, 2015; Owens *et al.*, 1993). Our study is the first to investigate the potential for dilbit biodegradation in shallow groundwater systems and represents one of longest-duration exposures to be run to date.

We were able to definitively demonstrate dilbit biodegradation in shallow groundwater mesocosms. By running side-by-side exposures under identical conditions, we directly compared the biodegradation potential of dilbit and a conventional heavy crude oil. In doing so, we address the key uncertainty of whether unconventional oils, such as dilbit, are sufficiently different from conventional oils to warrant changes to regulations. Our results suggest that both dilbit and conventional heavy crude show a similar potential for natural attenuation. Our findings can therefore be used in the assessment of the environmental threat posed by different crude oil types. This in turn will inform the development of more effective spill-response strategies.

References

Ahad, J., Burns, L., Mancini, S., and Slater, G. (2010a). Assessing Microbial Uptake of Petroleum Hydrocarbons in Groundwater Systems Using Natural Abundance Radiocarbon. Environmental science & technology *44*, 5092-5097. 10.1021/es100080c.

Ahad, J.M., Burns, L., Mancini, S., and Slater, G.F. (2010b). Assessing microbial uptake of petroleum hydrocarbons in groundwater systems using natural abundance radiocarbon. Environmental science & technology *44*, 5092-5097.

Ahad, J.M.E., and Pakdel, H. (2013). Direct Evaluation of in Situ Biodegradation in Athabasca Oil Sands Tailings Ponds Using Natural Abundance Radiocarbon. Environmental Science & Technology *47*, 10214-10222. 10.1021/es402302z.

Ahad, J.M.E., Pakdel, H., Gammon, P.R., Mayer, B., Savard, M.M., Peru, K.M., and Headley, J.V. (2020). Distinguishing Natural from Anthropogenic Sources of Acid Extractable Organics in Groundwater near Oil Sands Tailings Ponds. Environmental Science & Technology *54*, 2790-2799. 10.1021/acs.est.9b06875.

Ahad, J.M.E., Pakdel, H., Gammon, P.R., Siddique, T., Kuznetsova, A., and Savard, M.M. (2018). Evaluating in situ biodegradation of 13C-labelled naphthenic acids in groundwater near oil sands tailings ponds. Science of The Total Environment *643*, 392-399. https://doi.org/10.1016/j.scitotenv.2018.06.159.

Ahad, J.M.E., Pakdel, H., Labarre, T., Cooke, C.A., Gammon, P.R., and Savard, M.M. (2021). Isotopic Analyses Fingerprint Sources of Polycyclic Aromatic Compound-Bearing Dust in Athabasca Oil Sands Region Snowpack. Environmental Science & Technology *55*, 5887-5897. 10.1021/acs.est.0c08339.

Atlas, R.M. (1981). Microbial degradation of petroleum hydrocarbons: an environmental perspective. Microbiological reviews *45*, 180-209.

Atlas, R.M., and Hazen, T.C. (2011). Oil Biodegradation and Bioremediation: A Tale of the Two Worst Spills in U.S. History. Environmental Science & Technology *45*, 6709-6715. 10.1021/es2013227.

Atlas, R.M., Stoeckel, D.M., Faith, S.A., Minard-Smith, A., Thorn, J.R., and Benotti, M.J. (2015). Oil Biodegradation and Oil-Degrading Microbial Populations in Marsh Sediments Impacted by Oil from the Deepwater Horizon Well Blowout. Environmental Science & Technology *49*, 8356-8366. 10.1021/acs.est.5b00413.

Bastida, F., Jehmlich, N., Lima, K., Morris, B.E.L., Richnow, H.H., Hernández, T., von Bergen, M., and García, C. (2016). The ecological and physiological responses of the microbial community from a semiarid soil to hydrocarbon contamination and its bioremediation using compost amendment. Journal of Proteomics *135*, 162-169. https://doi.org/10.1016/j.jprot.2015.07.023.

Blair, N., Leu, A., Mu□oz, E., Olsen, J., Kwong, E., and Marais, D.D. (1985). Carbon isotopic fractionation in heterotrophic microbial metabolism. Applied and Environmental Microbiology *50*, 996-1001. doi:10.1128/aem.50.4.996-1001.1985.

Bolyen, E., Rideout, J.R., Dillon, M.R., Bokulich, N.A., Abnet, C.C., Al-Ghalith, G.A., Alexander, H., Alm, E.J., Arumugam, M., Asnicar, F., et al. (2019). Reproducible, interactive, scalable and extensible microbiome data science using QIIME 2. Nature Biotechnology *37*, 852-857. 10.1038/s41587-019-0209-9.

Caporaso, J.G., Lauber, C.L., Walters, W.A., Berg-Lyons, D., Huntley, J., Fierer, N., Owens, S.M., Betley, J., Fraser, L., and Bauer, M. (2012). Ultra-high-throughput microbial community analysis on the Illumina HiSeq and MiSeq platforms. The ISME journal *6*, 1621-1624.

CAPP (2020). 2019 Crude Oil Forecast, Markets and Transportation. Canadian Association of Petroleum Producers.

Carpenter, S.R. (1998). The Need for Large-Scale Experiments to Assess and Predict the Response of Ecosystems to Perturbation. In Successes, Limitations, and Frontiers in Ecosystem Science, M.L. Pace, and P.M. Groffman, eds. (Springer New York), pp. 287-312. 10.1007/978-1-4612-1724-4_12.

Cederwall, J., Black, T.A., Blais, J.M., Hanson, M.L., Hollebone, B.P., Palace, V.P., Rodríguez-Gil, J.L., Greer, C.W., Maynard, C., Ortmann, A.C., et al. (2020). Life under an oil slick: response of a freshwater food web to simulated spills of diluted bitumen in field mesocosms. Canadian Journal of Fisheries and Aquatic Sciences *77*, 779-788. 10.1139/cjfas-2019-0224.

Cowie, B.R., Greenberg, B.M., and Slater, G.F. (2010). Determination of Microbial Carbon Sources and Cycling during Remediation of Petroleum Hydrocarbon Impacted Soil Using Natural Abundance 14C Analysis of PLFA. Environmental Science & Technology *44*, 2322-2327. 10.1021/es9029717.

Crosby, S., Fay, R., Groark, C., Kani, A., Smith, J., Sullivan, T., Pavia, R., and Shigenaka, G. (2013). Transporting Alberta Oil Sands Products: Defining the Issues and Assessing the Risks 10.13140/2.1.1893.0240.

Davoodi, S.M., Miri, S., Taheran, M., Brar, S.K., Galvez-Cloutier, R., and Martel, R. (2020). Bioremediation of Unconventional Oil Contaminated Ecosystems under Natural and Assisted Conditions: A Review. Environmental Science & Technology *54*, 2054-2067. 10.1021/acs.est.9b00906.

Deshpande, R.S., Sundaravadivelu, D., Campo, P., SantoDomingo, J.W., and Conmy, R.N. (2017). Comparative Study on Rate of Biodegradation of Diluted Bitumen and Conventional Oil in Fresh Water. International Oil Spill Conference Proceedings *2017*, 2256-2267. 10.7901/2169-3358-2017.1.2256.

Deshpande, R.S., Sundaravadivelu, D., Techtmann, S., Conmy, R.N., Santo Domingo, J.W., and Campo, P. (2018). Microbial degradation of Cold Lake Blend and Western Canadian select dilbits by freshwater enrichments. J Hazard Mater *352*, 111-120. 10.1016/j.jhazmat.2018.03.030.

Dollhopf, R.H., Fitzpatrick, F.A., Kimble, J.W., Capone, D.M., Graan, T.P., Zelt, R.B., and Johnson, R. (2014). Response to Heavy, Non-Floating Oil Spilled in a Great Lakes River Environment: A Multiple-Lines-Of-Evidence Approach for Submerged Oil Assessment and Recovery. International Oil Spill Conference Proceedings *2014*, 434-448. 10.7901/2169-3358-2014.1.434.

Essaid, H.I., Bekins, B.A., Godsy, E.M., Warren, E., Baedecker, M.J., and Cozzarelli, I.M. (1995). Simulation of aerobic and anaerobic biodegradation processes at a crude oil spill site. Water Resources Research *31*, 3309-3327.

Essaid, H.I., Bekins, B.A., Herkelrath, W.N., and Delin, G.N. (2011). Crude oil at the bemidji site: 25 years of monitoring, modeling, and understanding. Ground Water *49*, 706-726. 10.1111/j.1745-6584.2009.00654.x.

Everett, L.G., and McMillion, L.G. (1985). Operational ranges for suction lysimeters. Groundwater Monitoring & Remediation *5*, 51-60.

Ferguson, D.K., Li, C., Jiang, C., Chakraborty, A., Grasby, S.E., and Hubert, C.R.J. (2020). Natural attenuation of spilled crude oil by cold-adapted soil bacterial communities at a decommissioned High Arctic oil well site. Science of The Total Environment *722*, 137258. https://doi.org/10.1016/j.scitotenv.2020.137258.

Fuentes, S., Méndez, V., Aguila, P., and Seeger, M. (2014). Bioremediation of petroleum hydrocarbons: catabolic genes, microbial communities, and applications. Applied Microbiology and Biotechnology *98*, 4781-4794. 10.1007/s00253-014-5684-9.

Government of Canada (2016). Oil Sands - Economic Contributions.

Green, C.T., and Scow, K.M. (2000). Analysis of phospholipid fatty acids (PLFA) to characterize microbial communities in aquifers. Hydrogeology Journal *8*, 126-141.

Greenwood, P.F., Wibrow, S., George, S.J., and Tibbett, M. (2009). Hydrocarbon biodegradation and soil microbial community response to repeated oil exposure. Organic Geochemistry *40*, 293-300.

Guckert, J.B., Antworth, C.P., Nichols, P.D., and White, D.C. (1985). Phospholipid, ester-linked fatty acid profiles as reproducible assays for changes in prokaryotic community structure of estuarine sediments*. FEMS Microbiology Letters *31*, 147-158. 10.1111/j.1574-6968.1985.tb01143.x.

Hamamura, N., Olson, S.H., Ward, D.M., and Inskeep, W.P. (2006). Microbial Population Dynamics Associated with Crude-Oil Biodegradation in Diverse Soils. Applied and Environmental Microbiology *72*, 6316-6324. doi:10.1128/AEM.01015-06.

Hanson, B.T., Yagi, J.M., Jeon, C.O., and Madsen, E.M. (2012). Role of nitrogen fixation in the autecology of Polaromonas naphthalenivorans in contaminated sediments. Environmental Microbiology *14*, 1544-1557. https://doi.org/10.1111/j.1462-2920.2012.02743.x.

Hayes, J.M. (2001). Fractionation of Carbon and Hydrogen Isotopes in Biosynthetic Processes*. Reviews in Mineralogy and Geochemistry *43*, 225-277. 10.2138/gsrmg.43.1.225.

Hayes, J.M. (2018). 3. Fractionation of Carbon and Hydrogen Isotopes in Biosynthetic Processes. Stable isotope geochemistry, 225-278.

Hazen, T.C., Prince, R.C., and Mahmoudi, N. (2016). Marine Oil Biodegradation. Environmental Science & Technology *50*, 2121-2129. 10.1021/acs.est.5b03333.

Hossain, S.Z., Mumford, K.G., and Rutter, A. (2017). Laboratory study of mass transfer from diluted bitumen trapped in gravel. Environmental Science: Processes & Impacts *19*, 1583-1593.

Hua, Y., Mirnaghi, F.S., Yang, Z., Hollebone, B.P., and Brown, C.E. (2018). Effect of evaporative weathering and oil-sediment interactions on the fate and behavior of diluted bitumen in marine environments. Part 1. Spill-related properties, oil buoyancy, and oil-particulate aggregates characterization. Chemosphere *191*, 1038-1047. https://doi.org/10.1016/j.chemosphere.2017.10.156.

Huang, J., Stoyanov, S.R., and Zeng, H. (2019). A comparison study on adsorption and interaction behaviors of diluted bitumen and conventional crude oil on model mineral surface. Fuel *253*, 383-391. https://doi.org/10.1016/j.fuel.2019.05.011.

Jeon, C.O., Park, W., Padmanabhan, P., DeRito, C., Snape, J.R., and Madsen, E.L. (2003). Discovery of a bacterium, with distinctive dioxygenase, that is responsible for in situ biodegradation in contaminated sediment. Proceedings of the National Academy of Sciences *100*, 13591-13596. 10.1073/pnas.1735529100.

Kämpfer, P., Busse, H.-J., and Falsen, E. (2006). Polaromonas aquatica sp. nov., isolated from tap water. International Journal of Systematic and Evolutionary Microbiology *56*, 605-608. https://doi.org/10.1099/ijs.0.63963-0.

Kassambara, A. (2021). Pipe-Friendly Framework for Basic Statistical Tests [R Package Rstatix Version 0.7. 0]. February. https://mran. microsoft. com/web/packages/rstatix/index. html.

Katoh, K., Misawa, K., Kuma, K.i., and Miyata, T. (2002). MAFFT: a novel method for rapid multiple sequence alignment based on fast Fourier transform. Nucleic acids research *30*, 3059-3066.

Keresztesi, Á., Nita, I.-A., Boga, R., Birsan, M.-V., Bodor, Z., and Szép, R. (2020). Spatial and long-term analysis of rainwater chemistry over the conterminous United States. Environmental Research *188*, 109872. https://doi.org/10.1016/j.envres.2020.109872.

King, T., Mason, J., Thamer, P., Wohlgeschaffen, G., Lee, K., and Clyburne, J. (2017). Composition of bitumen blends relevant to ecological impacts and spill response. pp. 463-475.

King, T., Robinson, B., McIntyre, C., Toole, P., Ryan, S., Saleh, F., Boufadel, M., and Lee, K. (2015). Fate of Surface Spills of Cold Lake Blend Diluted Bitumen Treated with Dispersant and Mineral Fines in a Wave Tank. Environmental Engineering Science *32*, 150127063128008. 10.1089/ees.2014.0459.

King, T.L., Robinson, B., Boufadel, M., and Lee, K. (2014). Flume tank studies to elucidate the fate and behavior of diluted bitumen spilled at sea. Marine Pollution Bulletin *83*, 32-37. https://doi.org/10.1016/j.marpolbul.2014.04.042.

Koehler, G., and Wassenaar, L.I. (2010). The stable isotopic composition (37Cl/35Cl) of dissolved chloride in rainwater. Applied Geochemistry *25*, 91-96. https://doi.org/10.1016/j.apgeochem.2009.10.004.

Kramer, C., and Gleixner, G. (2008). Soil organic matter in soil depth profiles: Distinct carbon preferences of microbial groups during carbon transformation. Soil Biology and Biochemistry *40*, 425-433. https://doi.org/10.1016/j.soilbio.2007.09.016.

Kweon, O., Kim, S.-J., Holland, R.D., Chen, H., Kim, D.-W., Gao, Y., Yu, L.-R., Baek, S., Baek, D.-H., Ahn, H., and Cerniglia, C.E. (2011). Polycyclic Aromatic Hydrocarbon Metabolic Network in Mycobacterium vanbaaleniiPYR-1. Journal of Bacteriology *193*, 4326-4337. doi:10.1128/JB.00215-11.

Lee, K., Boufadel, M., Chen, B., Foght, J., Hodson, P., Swanson, S., and Venosa, A. (2015). Expert Panel Report on the Behaviour and Environmental Impacts of Crude Oil Released into Aqueous Environments. Royal Society of Canada.

Lee, K., Bugden, J., Cobanli, S.E., McIntyre, C., Ryan, S., Wohlgeschaffen, G., and King, T. (2012). UV- Epifluorescence Microscopy Analysis of Sediments Recovered from the Kalamazoo River 10.13140/RG.2.1.4526.9209.

Lewan, M.D., Warden, A., Dias, R.F., Lowry, Z.K., Hannah, T.L., Lillis, P.G., Kokaly, R.F., Hoefen, T.M., Swayze, G.A., Mills, C.T., et al. (2014). Asphaltene content and composition as a measure of Deepwater Horizon oil spill losses within the first 80days. Organic Geochemistry *75*, 54-60. https://doi.org/10.1016/j.orggeochem.2014.06.004.

Lewis, J., Martel, R., Trépanier, L., Ampleman, G., and Thiboutot, S. (2009). Quantifying the Transport of Energetic Materials in Unsaturated Sediments from Cracked Unexploded Ordnance. Journal of Environmental Quality *38*, 2229-2236. https://doi.org/10.2134/jeq2009.0019.

Li, X., Fan, F., Zhang, B., Zhang, K., and Chen, B. (2018). Biosurfactant enhanced soil bioremediation of petroleum hydrocarbons: Design of experiments (DOE) based system optimization and phospholipid fatty acid (PLFA) based microbial community analysis. International Biodeterioration & Biodegradation *132*, 216-225. https://doi.org/10.1016/j.ibiod.2018.04.009.

Liao, J., Wang, J., and Huang, Y. (2015). Bacterial community features are shaped by geographic location, physicochemical properties, and oil contamination of soil in main oil fields of China. Microbial ecology *70*, 380-389.

Liu, Q., Tang, J., Gao, K., Gurav, R., and Giesy, J.P. (2017). Aerobic degradation of crude oil by microorganisms in soils from four geographic regions of China. Scientific Reports *7*, 14856. 10.1038/s41598-017-14032-5.

Mahmoudi, N., Beaupré, S.R., Steen, A.D., and Pearson, A. (2017). Sequential bioavailability of sedimentary organic matter to heterotrophic bacteria. Environmental Microbiology *19*, 2629-2644. 10.1111/1462-2920.13745.

Mahmoudi, N., Fulthorpe, R.R., Burns, L., Mancini, S., and Slater, G.F. (2013a). Assessing microbial carbon sources and potential PAH degradation using natural abundance 14C analysis. Environ Pollut *175*, 125-130. 10.1016/j.envpol.2012.12.020.

Mahmoudi, N., Porter, T.M., Zimmerman, A.R., Fulthorpe, R.R., Kasozi, G.N., Silliman, B.R., and Slater, G.F. (2013b). Rapid Degradation of Deepwater Horizon Spilled Oil by Indigenous Microbial Communities in Louisiana Saltmarsh Sediments. Environmental Science & Technology *47*, 13303-13312. 10.1021/es4036072.

Margesin, R., Hämmerle, M., and Tscherko, D. (2007). Microbial activity and community composition during bioremediation of diesel-oil-contaminated soil: effects of hydrocarbon concentration, fertilizers, and incubation time. Microbial Ecology *53*, 259-269.

McGill University (2022). Gault Nature Reserve. https://www.mcgill.ca/historicalcollections/gault.

McGowan, E., Song, L., and Hasemyer, D. (2012). The Dilbit Disaster: Inside the Biggest Oil Spill You've Never Heard Of (InsideClimate News).

McMurdie, P.J., and Holmes, S. (2013). phyloseq: an R package for reproducible interactive analysis and graphics of microbiome census data. PloS one *8*, e61217.

Miller, J.I., Techtmann, S., Fortney, J., Mahmoudi, N., Joyner, D., Liu, J., Olesen, S., Alm, E., Fernandez, A., Gardinali, P., et al. (2019). Oil Hydrocarbon Degradation by Caspian Sea Microbial Communities. Frontiers in Microbiology *10*. 10.3389/fmicb.2019.00995.

National Academies of Sciences, Engineering and Medicine, (2016). Spills of diluted bitumen from pipelines: a comparative study of environmental fate, effects, and response.

National Sanitation Foundation (NSF) International (2016). NSF International Standard/American National Standard for Drinking Water Additives NSF/ANSI 60 - 2016 Drinking water treatment chemicals - Health effects. NSF International.

Ng, G.-H., Bekins, B., Cozzarelli, I., Baedecker, M., Bennett, P., Amos, R., and Herkelrath, W. (2015). Reactive transport modeling of geochemical controls on secondary water quality impacts at a crude oil spill site near Bemidji, MN. Water Resources Research *51*. 10.1002/2015WR016964.

NRCan (2020). Crude Oil Facts. https://www.nrcan.gc.ca/science-data/data-analysis/energy-data-analysis/energy-facts/crude-oil-facts/20064#shr-pg0.

Oksanen, J., Blanchet, F.G., Kindt, R., Legendre, P., Minchin, P.R., O'hara, R., Simpson, G.L., Solymos, P., Stevens, M.H.H., and Wagner, H. (2013). Package 'vegan'. Community ecology package, version *2*, 1-295.

Ortmann, A.C., Cobanli, S.E., Wohlgeschaffen, G., MacDonald, J., Gladwell, A., Davis, A., Robinson, B., Mason, J., and King, T.L. (2020). Measuring the fate of different diluted bitumen products in coastal surface waters. Marine Pollution Bulletin *153*, 111003. https://doi.org/10.1016/j.marpolbul.2020.111003.

Ortmann, A.C., Cobanli, S.E., Wohlgeschaffen, G., Thamer, P., McIntyre, C., Mason, J., and King, T.L. (2019). Inorganic nutrients have a significant, but minimal, impact on a coastal microbial community's response to fresh diluted bitumen. Marine Pollution Bulletin *139*, 381-389. https://doi.org/10.1016/j.marpolbul.2019.01.012.

Owens, E., Taylor, E., Marty, R., and Little, D. (1993). An inland oil spill response manual to minimize adverse environmental impacts. In 1. (American Petroleum Institute), pp. 105-109.

Parks, D.H., Chuvochina, M., Waite, D.W., Rinke, C., Skarshewski, A., Chaumeil, P.-A., and Hugenholtz, P. (2018). A standardized bacterial taxonomy based on genome phylogeny substantially revises the tree of life. Nature Biotechnology *36*, 996-1004. 10.1038/nbt.4229.

Pérez-Pantoja, D., Donoso, R., Agulló, L., Córdova, M., Seeger, M., Pieper, D.H., and González, B. (2012). Genomic analysis of the potential for aromatic compounds biodegradation

in Burkholderiales. Environmental Microbiology *14*, 1091-1117. https://doi.org/10.1111/j.1462-2920.2011.02613.x.

Pesarini, P.F., de Souza, R.G.S., Corrêa, R.J., Nicodem, D.E., and de Lucas, N.C. (2010). Asphaltene concentration and compositional alterations upon solar irradiation of petroleum. Journal of Photochemistry and Photobiology A: Chemistry *214*, 48-53. https://doi.org/10.1016/j.jphotochem.2010.06.005.

Price, M.N., Dehal, P.S., and Arkin, A.P. (2010). FastTree 2–approximately maximum-likelihood trees for large alignments. PloS one *5*, e9490.

Quast, C., Pruesse, E., Yilmaz, P., Gerken, J., Schweer, T., Yarza, P., Peplies, J., and Glöckner, F.O. (2012). The SILVA ribosomal RNA gene database project: improved data processing and web-based tools. Nucleic Acids Research *41*, D590-D596. 10.1093/nar/gks1219.

R Core Team (2020). R: A language and environment for statistical computing (R Foundation for Statistical Computing, Vienna, Austria).

Radović, J.R., Oldenburg, T.B.P., and Larter, S.R. (2018). Chapter 19 - Environmental Assessment of Spills Related to Oil Exploitation in Canada's Oil Sands Region. In Oil Spill Environmental Forensics Case Studies, S.A. Stout, and Z. Wang, eds. (Butterworth-Heinemann), pp. 401-417. https://doi.org/10.1016/B978-0-12-804434-6.00019-7.

Ramseur, J.L., Lattanzio, R.K., Luther, L., Parfamak, P.W., and Cater, N.T. (2012). Oil sands and the Keystone XL pipeline: Background and selected environmental issues. Congressional Research Service Report - R42611, 1-62.

Rees, H.C., Oswald, S.E., Banwart, S.A., Pickup, R.W., and Lerner, D.N. (2007). Biodegradation Processes in a Laboratory-Scale Groundwater Contaminant Plume Assessed by Fluorescence Imaging and Microbial Analysis. Applied and Environmental Microbiology *73*, 3865. 10.1128/AEM.02933-06.

Rodgers-Vieira, E.A., Zhang, Z., Adrion, A.C., Gold, A., and Aitken, M.D. (2015). Identification of anthraquinone-degrading bacteria in soil contaminated with polycyclic aromatic hydrocarbons. Applied and environmental microbiology *81*, 3775-3781. 10.1128/AEM.00033-15.

Schindler, D.W. (1998). Whole-ecosystem experiments: replication versus realism: the need for ecosystem-scale experiments. Ecosystems *1*, 323-334.

Schreiber, L., Fortin, N., Tremblay, J., Wasserscheid, J., Elias, M., Mason, J., Sanschagrin, S., Cobanli, S., King, T., Lee, K., and Greer, C.W. (2019). Potential for Microbially Mediated Natural Attenuation of Diluted Bitumen on the Coast of British Columbia (Canada). Applied and Environmental Microbiology *85*, e00086-00019. 10.1128/AEM.00086-19.

Schreiber, L., Fortin, N., Tremblay, J., Wasserscheid, J., Sanschagrin, S., Mason, J., Wright, C.A., Spear, D., Johannessen, S.C., Robinson, B., et al. (2021). In situ microcosms deployed at the coast of British Columbia (Canada) to study dilbit weathering and associated microbial communities under marine conditions. FEMS Microbiology Ecology *97*. 10.1093/femsec/fiab082.

Sizova, M., and Panikov, N. (2007). Polaromonas hydrogenivorans sp. nov., a psychrotolerant hydrogen-oxidizing bacterium from Alaskan soil. International Journal of Systematic and Evolutionary Microbiology *57*, 616-619. https://doi.org/10.1099/ijs.0.64350-0.

Slater, G.F., White, H.K., Eglinton, T.I., and Reddy, C.M. (2005). Determination of Microbial Carbon Sources in Petroleum Contaminated Sediments Using Molecular 14C Analysis. Environmental Science & Technology *39*, 2552-2558. 10.1021/es048669j.

Spalding, R.F., and Hirsh, A.J. (2012). Risk-Managed Approach for Routing Petroleum Pipelines: Keystone XL Pipeline, Nebraska. Environmental Science & Technology *46*, 12754-12758. 10.1021/es303238z.

Stoyanovich, S.S., Yang, Z., Hanson, M., Hollebone, B.P., Orihel, D.M., Palace, V., Rodriguez-Gil, J.L., Faragher, R., Mirnaghi, F.S., Shah, K., and Blais, J.M. (2019). Simulating a Spill of Diluted Bitumen: Environmental Weathering and Submergence in a Model Freshwater System. Environmental Toxicology and Chemistry *38*, 2621-2628. 10.1002/etc.4600.

Strausz, O.P., and Lown, E.M. (2003). The chemistry of Alberta oil sands, bitumens and heavy oils (Alberta Energy Research Institute Calgary, AB).

Stuiver, M., and Polach, H.A. (1977). Discussion Reporting of 14C Data. Radiocarbon *19*, 355-363. 10.1017/S0033822200003672.

Sun, W., Dong, Y., Gao, P., Fu, M., Ta, K., and Li, J. (2015). Microbial communities inhabiting oil-contaminated soils from two major oilfields in Northern China: Implications for active petroleum-degrading capacity. J Microbiol *53*, 371-378. 10.1007/s12275-015-5023-6.

Turnbull, J.C., Lehman, S.J., Miller, J.B., Sparks, R.J., Southon, J.R., and Tans, P.P. (2007). A new high precision 14CO2 time series for North American continental air. Journal of Geophysical Research: Atmospheres *112*.

Vázquez, S., Monien, P., Pepino Minetti, R., Jürgens, J., Curtosi, A., Villalba Primitz, J., Frickenhaus, S., Abele, D., Mac Cormack, W., and Helmke, E. (2017). Bacterial communities and chemical parameters in soils and coastal sediments in response to diesel spills at Carlini Station, Antarctica. Science of The Total Environment *605-606*, 26-37. https://doi.org/10.1016/j.scitotenv.2017.06.129.

Vet, R., Artz, R.S., Carou, S., Shaw, M., Ro, C.-U., Aas, W., Baker, A., Bowersox, V.C., Dentener, F., Galy-Lacaux, C., et al. (2014). A global assessment of precipitation chemistry and deposition of sulfur, nitrogen, sea salt, base cations, organic acids, acidity and pH, and phosphorus. Atmospheric Environment *93*, 3-100. https://doi.org/10.1016/j.atmosenv.2013.10.060.

White, D.C., Davis, W.M., Nickels, J.S., King, J.D., and Bobbie, R.J. (1979). Determination of the sedimentary microbial biomass by extractible lipid phosphate. Oecologia *40*, 51-62. 10.1007/BF00388810.

Wickham, H. (2011). ggplot2. WIREs Computational Statistics *3*, 180-185. https://doi.org/10.1002/wics.147.

Widdel, F., Knittel, K., and Galushko, A. (2010). Anaerobic hydrocarbon-degrading microorganisms: an overview. Handbook of hydrocarbon and lipid microbiology, 1998-2022.

Wilkinson, S., and Ratledge, C. (1988). Microbial lipids (Academic Press).

Yang, S., Wen, X., Shi, Y., Liebner, S., Jin, H., and Perfumo, A. (2016). Hydrocarbon degraders establish at the costs of microbial richness, abundance and keystone taxa after crude oil contamination in permafrost environments. Scientific Reports *6*, 37473. 10.1038/srep37473.

Zhao, J., Verma, M., and Verter, V. (2021). Pipeline transportation of crude oil in Canada: Environmental risk assessment using modified diffusion models. Human and Ecological Risk Assessment: An International Journal *27*, 1206-1226. 10.1080/10807039.2020.1816808.

Supporting Information

Table S1. Summary of samples collected during the mesocosm experiment that ran from August 2nd, 2019 to November 14th, 2019. In addition to the control, a dilbit treatment (DB) and a heavy conventional crude treatment (CC) were used in this study. Day 0 samples were taken prior to the addition of the DB and CC treatments.

Sample	Day	Depth (cm)	Treatment
1	0	0 – 15.24	Control
2	0	15.24 – 30.48	Control
3	0	30.48 – 45.72	Control
4	0	0 – 15.24	DB (prior to treatment)
5	0	15.24 – 30.48	DB (prior to treatment)
6	0	30.48 – 45.72	DB (prior to treatment)
7	0	0 – 15.24	CC (prior to treatment)
8	0	15.24 – 30.48	CC (prior to treatment)
9	0	30.48 – 45.72	CC (prior to treatment)
10	6	0 – 15.24	Control
11	6	15.24 – 30.48	Control
12	6	30.48 – 45.72	Control
13	6	0 – 15.24	DB
14	6	15.24 – 30.48	DB
15	6	30.48 – 45.72	DB
16	6	0 – 15.24	CC
17	6	15.24 – 30.48	CC
18	6	30.48 – 45.72	CC
19	13	0 – 15.24	Control
20	13	15.24 – 30.48	Control
21	13	30.48 – 45.72	Control
22	13	0 – 15.24	DB
23	13	15.24 – 30.48	DB
24	13	30.48 – 45.72	DB
25	13	0 – 15.24	CC
26	13	15.24 – 30.48	CC
27	13	30.48 – 45.72	CC
28	21	0 – 15.24	Control
29	21	15.24 – 30.48	Control
30	21	30.48 – 45.72	Control
31	21	0 – 15.24	DB
32	21	15.24 – 30.48	DB
33	21	30.48 – 45.72	DB
34	21	0 – 15.24	CC
35	21	15.24 – 30.48	CC
36	21	30.48 – 45.72	CC
37	34	0 – 15.24	Control
38	34	15.24 – 30.48	Control
39	34	30.48 – 45.72	Control

40	34	0 – 15.24	DB
41	34	15.24 – 30.48	DB
42	34	30.48 – 45.72	DB
43	34	0 – 15.24	CC
44	34	15.24 – 30.48	CC
45	34	30.48 – 45.72	CC
46	48	0 – 15.24	Control
47	48	15.24 – 30.48	Control
48	48	30.48 – 45.72	Control
49	48	0 – 15.24	DB
50	48	15.24 – 30.48	DB
51	48	30.48 – 45.72	DB
52	48	0 – 15.24	CC
53	48	15.24 – 30.48	CC
54	48	30.48 – 45.72	CC
55	62	0 – 15.24	Control
56	62	15.24 – 30.48	Control
57	62	30.48 – 45.72	Control
58	62	0 – 15.24	DB
59	62	15.24 – 30.48	DB
60	62	30.48 – 45.72	DB
61	62	0 – 15.24	CC
62	62	15.24 – 30.48	CC
63	62	30.48 – 45.72	CC
64	76	0 – 15.24	Control
65	76	15.24 – 30.48	Control
66	76	30.48 – 45.72	Control
67	76	0 – 15.24	DB
68	76	15.24 – 30.48	DB
69	76	30.48 – 45.72	DB
70	76	0 – 15.24	CC
71	76	15.24 – 30.48	CC
72	76	30.48 – 45.72	CC
73	90	0 – 15.24	Control
74	90	15.24 – 30.48	Control
75	90	30.48 – 45.72	Control
76	90	0 – 15.24	DB
77	90	15.24 – 30.48	DB
78	90	30.48 – 45.72	DB
79	90	0 – 15.24	CC
80	90	15.24 – 30.48	CC
81	90	30.48 – 45.72	CC
82	104	0 – 15.24	Control
83	104	15.24 – 30.48	Control
84	104	30.48 – 45.72	Control
85	104	0 – 15.24	DB

86	104	15.24 – 30.48	DB
87	104	30.48 – 45.72	DB
88	104	0 – 15.24	CC
89	104	15.24 – 30.48	CC
90	104	30.48 – 45.72	CC

Table S2. Radiocarbon ($\Delta^{14}C$) values for bulk PLFAs and fraction of PLFA carbon derived from soil organic matter (SOM) and oil on Days 0, 34, 62, and 104. Top, middle and bottom sampling depths were combined for Days 0 (Control) and 104 (Control, dilbit and heavy conventional crude). Top, middle, and bottom sampling depths were analysed individually for Days 34 and 64 samples.

Day	Depth	Treatment	$\Delta^{14}C$	SOM Fraction	Oil Fraction
0	Combined	Control	17.4	1	0
34	Top	Conventional Crude	-153.4	0.8695	0.1305
34	Middle	Conventional Crude	-99.6	0.9248	0.0752
34	Bottom	Conventional Crude	-174.8	0.8475	0.1525
34	Top	Dilbit	-195.9	0.8258	0.1742
34	Middle	Dilbit	-46.8	0.9792	0.0208
34	Bottom	Dilbit	-107.3	0.917	0.083
62	Top	Conventional Crude	-253.2	0.7668	0.2332
62	Middle	Conventional Crude	-100.1	0.9243	0.0757
62	Bottom	Conventional Crude	-90.4	0.9344	0.0656
62	Top	Dilbit	-215.6	0.8054	0.1946
62	Middle	Dilbit	-202.3	0.8192	0.1808
62	Bottom	Dilbit	-187.3	0.8346	0.1654
104	Combined	Conventional Crude	-194.2	0.8275	0.1725
104	Combined	Control	8.7	1	0
104	Combined	Dilbit	-213	0.8082	0.1918